International Journal of
Young Scientist Research

Vol 4, No1, Dec 2020
ISSN: 2588- 5111

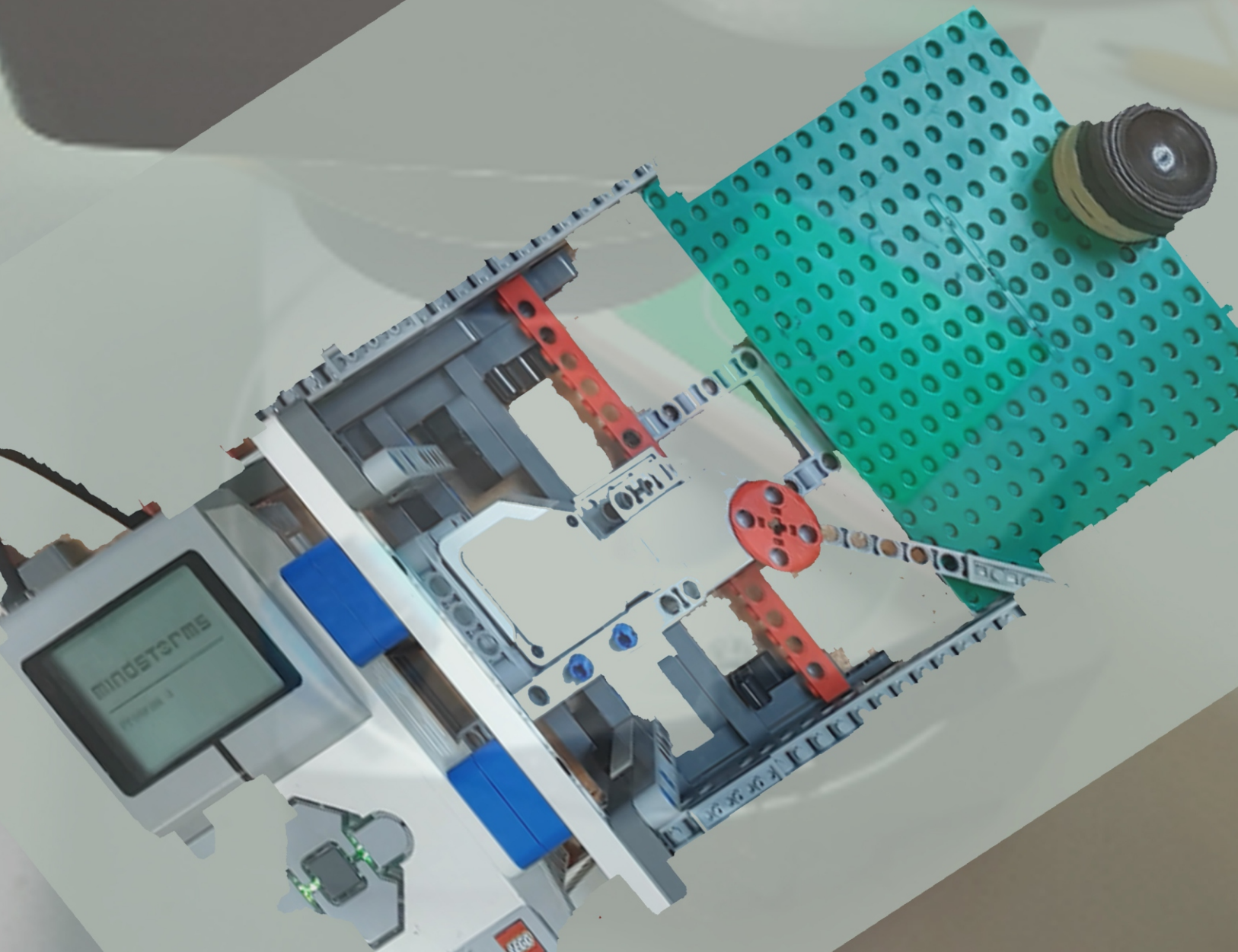

Contents

Young Scientist Research

Address:
Unit 14, No.32, Malek Ave., Shariati St.
Post Code: 1565843537
Tel:+9821-77507013, 77522395

WELCOME TO THE INTERNATIONAL JOURNAL of YOUNG SCIENTIST RESEARCH

Young Scientist Research is a research journal based on scientific projects and we are pleased to present our students' work in scientific activities. This open-access journal includes young students' research in any field of science which publishes full-length and abstract research on any aspects of applied sciences in relation to work presented in both national and international conferences, competitions and tournaments of all types.

Programs that have educational opportunities for high school students to present their distinguished projects from regional, national and international events such as International Conference of Young Scientists (ICYS), International / Persian Young Physicists' Tournament (IYPT/ PYPT), International / Iran Physics' Tournament (IPT/ IRPT).

New manuscripts sent to the Journal will be handled by the Editorial Office who checks compliance with the guidelines to authors. Then a rapid screening process at which stage a decision to reject or to go to full review is made.

By submission of a manuscript to the Journal, all authors warrant that they have the authority to publish the material and that the paper, or one substantially the same, has neither been published previously, nor is being considered for publication elsewhere.

This journal belongs to Ariaian Young Innovative Minds Institute, AYIMI, and one to two issues is published in a year. All details are on the YOUNG SCIENTIST RESEARCH Journal website (http://journal. ayimi.org)

Editor in Chief
Dr. Dina Izadi
Researcher & President
AYIMI & ADIB
International Research & Artistic Institutes
http://www.ayimi.org, http://adib.ayimi.org
Email: info@ayimi.org
Unit 14, No. 32, Malek Ave., Shariati St.,
Post Code: 1565843537
Young Scientist Research Journal, ISSN: 2588-5111
http://journal.ayimi.org
Tehran/ Iran

CURRENT ISSUE
Vol 4 NO 1 DEC 2020

Investigation of Parameters in Oscillations of Newton's Cradle

Amirmehdi Jafari Fesharaki, Sharif University of Technology, amiroo23jf@gmail.com

ARTICLE INFO

IYPT 2019 Iran Team member in Poland and Winner of Bronze Medal

Accepted in country selection by Ariaian Young Innovative Minds Institute , AYIMI

http://www.ayimi.org , info@ayimi.org

ABSTRACT

This is a problem related to oscillations of a Newton's cradle which will gradually decay until the spheres come to the rest. The effect of several parameters such as number, material and alignment of the spheres on the rate of decay in this research have been investigated. The collision between two balls was our initial observation and then it was extended to a higher number of balls. A comparison between middle and side ball and the effect of number of the releasing balls and alignment are investigated theoretically which shows the decay in collisions and also increasing the number of the balls will cause increasing the rate of decay too. It also shows that as we use more elastic materials, the rate of decay decreases in our experiment.

Key Words: *oscillation, Newton's cradle, collision, elastic materials*

1 Introduction

Newton's cradle is constructed from a series of pendulums (usually five in number) abutting one another. Each pendulum is attached to a frame by two strings of equal length angled away from each other. If these strings were not same in length, the balls would then be unbalanced. This string arrangement restricts the pendulums' movements to the same plane. In Newton's cradle when the first ball is released, it hits the second ball then transfers its momentum and energy to the last ball through the middle balls. This process repeats in reverse until the spheres come to the rest and all of the energy is dissipated. The behavior of the pendulum follows from the conservation of momentum and kinetic energy only in the case of two pendulums (Fig.1) [1].

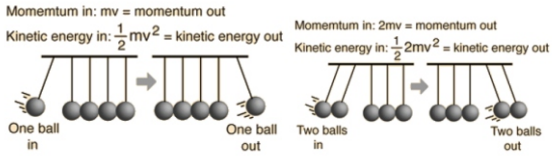

Fig.1: Demonstration of conservation of momentum and conservation of energy in Newton's cradle [2]

The phenomenon causes swinging pendulums to synchronize when they are close together, but if we have a number of pendulums, there are unknown parameters to be calculated from the initial conditions.

2 Materials, Devices and Method

2-1 Materials and Devices

When a ball on one end of the cradle is pulled away from the others and then released, it strikes the next ball in the cradle, which remains motionless. But the ball on the opposite end of the row is thrown into the air, then swings back to strike the other balls, starting the chain reaction again in reverse (Fig.2).

Two cradles in different materials, steel and copper, with 2 up to 5 number of balls, are used in this experiment.

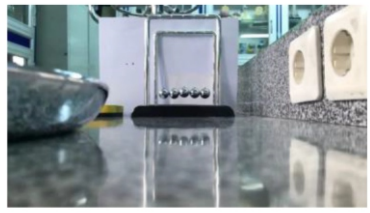

FIg 2: A Newton's Cradle setup

2-2 Methods and Modeling

This is started with modeling the collisions between two balls in the perfectly elastic condition. For perfectly elastic collision between two spheres, elasticity and ratio between two spheres' masses is equal to 1. When the first ball hits the second ball, all of its momentum and energy is transferred to the next ball and it starts moving with the first ball's initial velocity. When the first ball collides with the second, the first ball stops, and its momentum is transferred to the second ball until it reaches the last ball. In perfectly elastic collision between two balls, we have (Eq. 1) (Fig.3 a and b).

Full paper has been published in:

Lat. Am. J. Phys. Educ. Vol. 14, No. 3, Sept. 2020

http://www.lajpe.org

SAXON BOWL

Daniel Norouzi, danyu9046@gmail.com

ARTICLE INFO

O-IYPT 2020 Iran Team member and Winner of Gold Medal in national tournament, PYPT 2020

Accepted in country selection by Ariaian Young Innovative Minds Institute , AYIMI

http://www.ayimi.org ,info@ayimi.org

ABSTRACT

Saxon bowl is a bowl with a hole in its base that will sink when placed in water. In this paper, this phenomenon and the parameters that determine the time of submersion were investigated. Two differential equations were evaluated by neglecting some effects and parameters such as viscosity, water turbulence, etc. Then they were solved either by approximation and coding in Python programming language. While adjusting the vessel mass and hole area, total 54 experiments were conducted by adjusting one variable and keeping the other constant. It was observed that the experiment and modeling results differ but have a close trend because of the neglected parameters and effects.

Key Words: *Saxon Bowl, time measurement, sinking, numerical modeling*

1 Introduction

Saxon Bowl with a hole in its bottom placed in water by Saxons and the time it took the bowl to submerge was measured. The rate in which the bowl sinks depends on several parameters such as the flow rate of water through the hole, pressure, buoyancy, viscosity and etc. To investigate and analyze this phenomenon, experiment and modeling help us to find the submersion time as a function of these factors.

2 Theory and Modeling

The vessel can be modeled as a cylinder with height (L), base area (S) and hole area (A) (Fig. 1). The thickness of the vessel can be neglected. The sunk length of the vessel (h) and the height of water inside the vessel (x) are variables in respect to time.

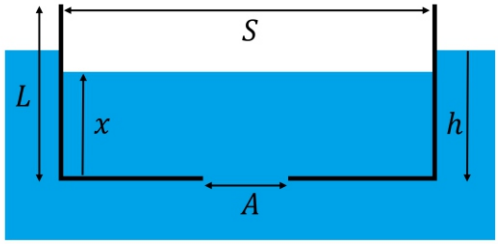

Fig. 1: Modeling of the vessel

To find the flow of water inside the vessel, viscosity of water is neglected and the Bernoulli's equation was used and we assume there's no turbulence in the water flow. Since we neglected the thickness of the vessel, the water viscosity can be neglected in the hole section. The average of parameters and their errors were found by the equations (1-4).

$$\bar{x} = \frac{\sum x_i}{n} \tag{1}$$

$$\Delta\bar{x} = \sqrt{\frac{\sum(x_i - \bar{x})^2}{n(n-1)}} = \frac{\sigma_n}{\sqrt{n-1}} \tag{2}$$

$$\Delta\bar{M}^{-0.5} = \frac{\Delta\bar{M}}{2\sqrt{\bar{M}^3}} \tag{3}$$

$$\Delta\bar{A} = \frac{\pi\bar{D}\Delta\bar{D}}{2} \tag{4}$$

With dimensional analysis, a dimensionless parameter (c) was evaluated which equals to 8.2×10^{-6}. Dimensional analysis shows that the water viscosity in the vessel is relatively small in respect to other parameters of the vessel, so its influence can be neglected (Eqs. 5-7).

$$C = \frac{\mu}{\rho_{water}\sqrt{g\sqrt{S^3}}} = 8.2\times10^{-6} \tag{5}$$

$$P + \rho_{fluid}gh + \frac{1}{2}\rho_{fluid}v^2 = Const. \quad (Bernoulli's\ equation) \tag{6}$$

$$Av = const. \quad (Equation\ of\ continuity) \tag{7}$$

In equations, P is the water pressure, h height in respect to ground, v the velocity of water and A is the pipe area.
The vessel is sinking inside a bigger vessel. The water flow is modeled as it's flowing from a very wide pipe (bigger vessel) into a smaller pipe (sinking vessel). Since the area of the first pipe is much wider than the second pipe, the equation of continuity concludes that its water flow velocity is relatively small in respect to the smaller pipe so we neglect the third term in the Bernoulli's equation. The third term of the equation for the sinking vessel is found by the water pressure difference at the entrance of the vessel which equals to the static pressure difference between the water inside the vessel with height (x) and the water inside the bigger vessel at depth (h). Moreover, since the sinking vessel is accelerating, the static water pressure inside the vessel decreases and the sinking velocity of the vessel itself is added to the water flow velocity at the entrance (Eqs. 8,9).

$$\frac{1}{2}\rho_{water}(v_{entrance} - \dot{h})^2 = \rho_{water}gh - \rho_{water}(g - \ddot{h})x \tag{8}$$

$$Av_{entrance} = S\dot{x} \tag{9}$$

With some substitutions, the rate of water flow inside the vessel is found (Eq. 10):

$$\frac{dx}{dt} = \frac{A}{S}\left(\sqrt{2(gh - (g - \ddot{h})x)} + \dot{h}\right) \tag{10}$$

buoyancy force, drag, and the change in momentum flux of water flow when it's entering the vessel from the hole (Eq. 11).

$$\vec{F} = M\vec{a} = \frac{d\vec{P}}{dt} \tag{11}$$

Since the density of the Polypropylene (PP) is nearly as water, the buoyancy force of the vessel material itself, cancels its weight. Coins were used to increase the mass of the vessel, which their density is more than water's density but the buoyancy force and the acceleration of the vessel itself, decreases the force they exert on the vessel. The buoyancy force that exerts on the system is found by the water pressure difference at the entrance of the vessel which equals to the static pressure difference between the water inside the vessel with height (x) and the water inside the bigger vessel at depth (h).

The drag force is found by equation (12) where C_D and *S-A* are the coefficient of drag and the projected area, respectively. The coefficient of drag was found from figure (2) which is the coefficient of drag in respect to the Reynolds number (Eq. 13).

$$F_D = \frac{1}{2} C_D \rho_{fluid} (S - A) v^2 \tag{12}$$

$$R_E = \frac{\rho_{fluid} v D}{\mu} \tag{13}$$

The Reynolds number for the vessel is approximately 700. So from figure (2), the coefficient of drag for the vessel is approximately 1.

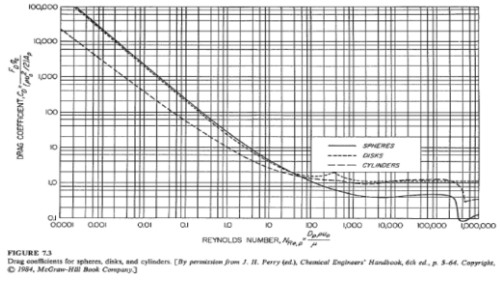

FIGURE 7.3
Drag coefficients for spheres, disks, and cylinders. [*By permission from J. H. Perry (ed.), Chemical Engineers' Handbook, 4th ed., p. 5-64. Copyright, © 1984, McGraw-Hill Book Company.*]

Fig.2: Coefficient of drag chart

Momentum flow for a stream of water is described as follows (Eq. 14):

$$\dot{\vec{P}} = \rho A v^2 \hat{v} \tag{14}$$

For the vessel, the momentum flows are (Eqs. 15-17):

$$\dot{\vec{P}}_{in} = \rho A (v_{entrance} - \dot{h})^2 \hat{z} \tag{15}$$

$$\dot{\vec{P}}_{out} = \rho S (\dot{x} - \dot{h})^2 \hat{z} \tag{16}$$

$$\vec{F} = \dot{\vec{P}}_{in} - \dot{\vec{P}}_{out} = \left(\frac{S}{A} \dot{x}^2 - \dot{h}^2 \right) (S - A) \hat{z} \tag{17}$$

Then Newton's second law will be (Eq. 18):

$$(M_{coins} + M_{vessel}) \ddot{h} = \left(1 - \frac{\rho_{water}}{\rho_{coin}}\right) M_{coins} (g - \ddot{h}) - \rho_{water} (S - A) \left((gh - (g - \ddot{h})x) - \frac{1}{2} \dot{h}^2 + \frac{S\dot{x}^2}{A} \right) \tag{18}$$

and the equations of the vessel are (Eqs. 19 , 20)

$$\dot{x} = \frac{A}{S} \left(\sqrt{2(gh - (g - \ddot{h})x)} + \dot{h} \right) \tag{19}$$

$$\ddot{h} = \frac{\left(1 - \frac{\rho_{water}}{\rho_{coin}}\right) M_{coins} g - \rho_{water} (S - A) \left(g(h - x) - \frac{1}{2} \dot{h}^2 + \frac{S\dot{x}^2}{A} \right)}{(M_{vessel} + \left(2 - \frac{\rho_{water}}{\rho_{coin}}\right) M_{coins} + \rho_{water} (S - A) x)} \tag{20}$$

3 Experiments

A 11.290 (g) Polypropylene (PP) vessel with the dimensions of 12 (D) * 8.5(H) (cm) and with a central hole was used. The weight of vessel was adjusted by adding coins on the base. The mass of the vessel and coins were measured by a balance with accuracy ± 0.001(g) , the time of submersion by a stopwatch with accuracy ± 0.01(s) and the vessel's dimensions by a ruler with accuracy ± 0.1(cm) (Fig. 3).

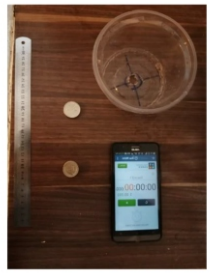

Fig. 3: Experimental setup

In this experiment, two variables of vessel mass and hole diameter were used, ranging from 31.530 to 88.984 (g) and 1.6 to 3.4 (cm), respectively. The method was placing the vessel so that the hole was just in contact with the water surface. The vessel was allowed to sink while the time of submersion was recorded until the surface of water reached the lip of the vessel.

To investigate the influence of various parameters i.e. vessel mass and hole diameter, while the hole diameter was 1.6 (cm), for 9 masses, 27 experiments and while the mass was 82.222(g), for 9 diameters, 27 experiments were conducted .

4 Results and Discussion

4-1 Solution I

The equations 19 and 20 are solved analytically with some approximations and simplifications. Since the vessel is sinking with low velocity, it is assumed that the changes in x and h parameters occur slowly, with the result that the system is always in (approximate) equilibrium. So it's concluded that the vessel is sinking with constant velocity and no acceleration (Eq. 21):

$$\begin{aligned} \ddot{h} &= \ddot{x} = 0 \\ \dot{x} &= \dot{h} = v = Const. \\ h - x &= \ell = Const. \end{aligned} \tag{21}$$

then:

$$v = \frac{A}{S - A} \sqrt{2g\ell} \tag{22}$$

$$\left(1 - \frac{\rho_{water}}{\rho_{coin}}\right) M_{coins} g = \rho_{water} (S - A) \left(g\ell + v^2 \left(\frac{S}{A} - \frac{1}{2}\right) \right) \tag{23}$$

$$\ell = \frac{(S - A) \left(1 - \frac{\rho_{water}}{\rho_{coin}}\right) M_{coins}}{\rho_{water} S^2} \tag{24}$$

$$v = \sqrt{\frac{2 \left(1 - \frac{\rho_{water}}{\rho_{coin}}\right) g M_{coins} A^2}{\rho_{water} (S - A) S^2}} \tag{25}$$

The height of the vessel is L, and the initial (t=0) value of h was found by buoyancy force of the system when there's no water in the vessel (equation 32). So the time of submersion T is as follows (Eqs. 26-27):

$$h_0 = \frac{M_{coins}}{S\rho_{water}} \tag{26}$$

$$T = \frac{L - h_0}{v} = \left(L - \frac{M_{coins}}{S\rho_{water}}\right)\sqrt{\frac{\rho_{water}(S-A)S^2}{2\left(1-\frac{\rho_{water}}{\rho_{coin}}\right)g}}\frac{1}{A\sqrt{M_{coins}}} \tag{27}$$

Assuming that the hole area is much smaller than the base area of the vessel $(S \gg A)$ and the initial value of h is much smaller than the height of the vessel $(L \gg h_0)$, the time of submersion is related to the hole area by A^{-1} and it's related to the coins mass by $M^{-0.5}$ (Eq. 28).

$$T \propto \frac{1}{A\sqrt{M_{coins}}} \tag{28}$$

The experiment results are plotted (Figs. 4 and 5). To investigate the conclusion of equation (28), the time of submersion was plotted as a function of $M^{-0.5}$ and A^{-1} which fitted the trend line with R-squared value of 0.98 and 0.94, respectively.

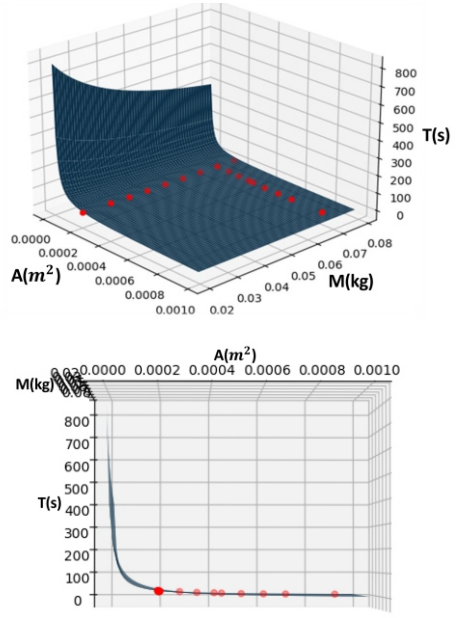

Fig. 4 and 5 : Time of submersion as a function of coins mass and hole area for solution (I) compared to experiments

and figures (6-9):

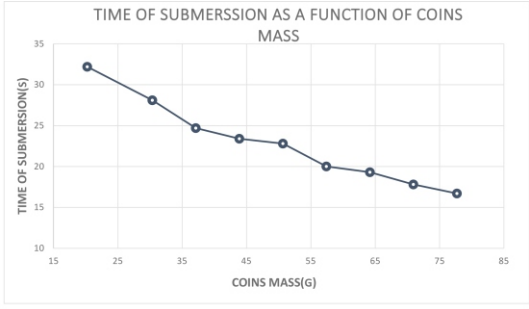

Fig. 6: Time of submersion as a function of coin's mass

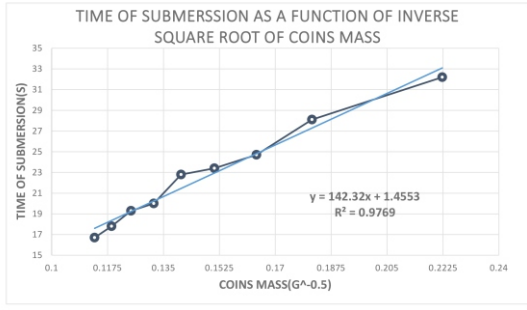

Fig. 7: Time of submersion as a function of inverse square root of coin's mass

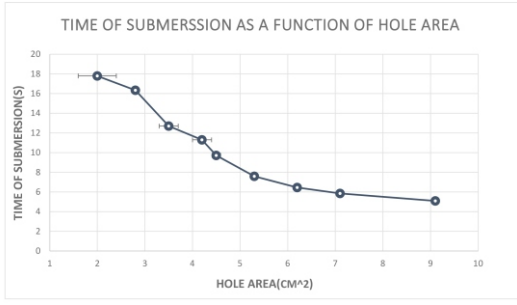

Fig. 8: Time of submersion as a function of hole area

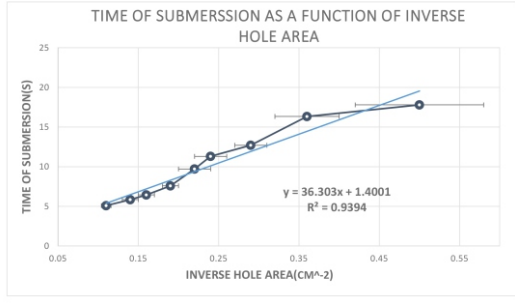

Fig. 9: Time of submersion as a function of inverse hole area

4-2 Solution II

Another way to solve the equations 19 and 20, is to solve them numerically. So Python programming language was used to write a code that solves the equations numerically. So the properties and initial conditions of the vessel should be defined in the code.

The code plots both vessel parameters x and h as a function of time. So the solution of the equations 19 and 20 and the vessel motion tracked by the Tracker program is as follows (Fig. 10):

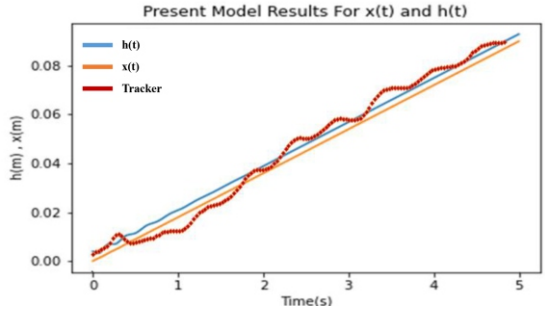

Fig. 10: The numerical solution for x(t) and h(t)

To find the submersion time as a function of hole area and coin's mass, syntaxes were added to the code to find the time where $\boldsymbol{h = 8.5\ (cm)}$ for each coin's mass or hole area and plot them as a function of coin's mass or hole area and then plot the experiment results, so they could be compared (Figs. 11 and 12):

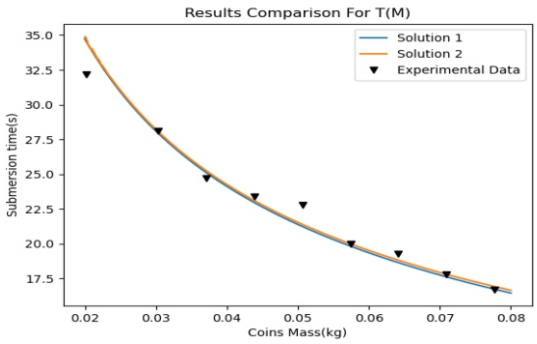

Fig. 11: Results comparison for submersion time as a function of coin's mass

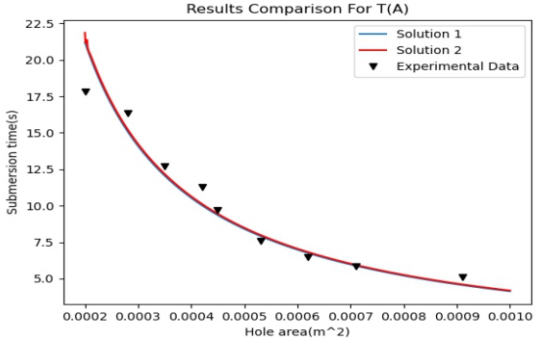

Fig. 12: Results comparison for submersion time as a function of hole area

4 Conclusion

The results show that the trend of the experiment results and the model results are close. In the modeling, some parameters and effects such as viscosity (ignored), coefficient of drag (approximated), water turbulence (ignored), water surface tension (ignored), etc. were neglected. So it's expected that the experiment and modeling results differ but have a close trend as it can be seen in the graphs.

References

[1] Kleppner, Kolenkow, An introduction to mechanics

[2] Halliday, Resnick, Walker, Fundamentals of physics

Determination of the Safe Dose of Euphorbia rigida Plant Extract to be used as Biopesticide, Antimicrobial and Antioxidant with Brine shrimp lethality assay

METIN MERT[a*] CENGİZ BEYZA[b] ONARAN MEHMET ALI[c]
a) Mugla Sıtkı Koçman University, Faculty of Milas Veterinary, Department of Biochemistry, 48200 Muğla, Turkey, mertmetin@mu.edu.tr
b) Muğla Private Yönelt Anatolian High School 12th Grade Science Student, 48100 Muğla, Turkey
c) Muğla Private Yönelt Anatolian High School Project Coordinator, 48100 Muğla, Turkey

ARTICLE INFO

This study is a part of a PhD thesis.

Corresponding author: METIN MERT

Winner of Gold Medal in IMSEF 2020, Turkey, Izmir and was awarded by Ariaian Young Innovative Minds Institute , AYIMI

http://www.ayimi.org ,info@ayimi.org

ABSTRACT

Euphorbia rigida Bieb. is a poisonous milk-bearing plant, which is in the form of shrubs or trees growing in tropical and temperate regions and belonging to the Euphorbiaceae family, which has nearly 100 species in our country. The Euphorbiaceae family, known for its capacity of being used as antioxidant, antimicrobial and biopecticides, has attracted great attention in recent years. In this study, the safe dose of the extracts of E. rigida Bieb. believed to have the capacity of being used in both medicinal and agricultural applications, and very common in Muğla, will be determined by using Brine shrimp lethality assay.

Key Words: *Euphorbia rigida, Brine shrimp lethality assay, Antimicrobial, Antioxidant, Biopestisit*

1 Introduction

Herbal products have been used since the Palaeolithic ages. It has been reported by the World Health Organization that 70-80% of the world population benefit from herbal products in basic health care applications (Sarışen and Çalışkan, 2005). The most important reason for the increasing interest in plant-based drugs is that although the synthesized chemical compounds used in the treatment of chronic diseases have limited effect, plant-based drugs are potentially more effective, cheaper, and have fewer side effects than synthetic drugs (Abay, 2006). As in the past, medicines obtained from plants or herbs are used in the treatment of various diseases today (Arıkan, 1992). In the modern world, human health and the environment have gained great importance. Many scientific studies point to the necessity of natural nutrition and the use of naturally derived antioxidants in order to stay healthy (Koca and Karadeniz, 2003). In addition, another factor that threatens human health is the incorrect use of chemicals in agricultural pest control. All kinds of residues of chemical pesticides used unconsciously in agricultural fields are mixed with soil, air and groundwater in various ways. Pesticides with high toxicity accumulate over time in all living creatures living in this environment and return to human through the food chain. Pesticides that return to humans by various means such as residues on the product or through the food chain threaten human health (cancer, genetic diseases etc.) (Özmen and Sümer, 2004). The main reason for refusing or returning agricultural products exported by our country is the presence of toxin or pesticide residues in our products. Increasing the export potential of our country is of great importance for our economic development. For this reason, it is very important to use herbal products for biopesticide purposes in agricultural pest control. According to a research conducted by the World Health Organization (WHO) based on some publications on medicinal plants of 91 countries, the total number of medicinal plants used for treatment purposes is around 20 000 (Çelik and Çelik, 2007). The number of medicinal plants used in our country is about 500 and it is very low compared to European countries, so it is necessary to benefit from our own natural herbal potential (Baytop, 2000). Most plant extracts have been used as topical antiseptics, or have been reported to have antimicrobial properties (Avcı et al., 2013). It is known that extracts and essential oils of naturally grown plants exhibit antibacterial and antifungal activity and provide the basis for many application areas such as antimicrobial activities, preservation of nutrients, as a biopesticide in agricultural control, pharmacy, alternative medicine and natural therapy (Çalışkan et al., 2019).

Euphorbia rigida Bieb. is a poisonous milk-bearing plant, which is in the form of shrubs or trees growing in tropical and temperate regions and belonging to the Euphorbiaceae family, which has nearly 100 species in our country our country and is used as a poison in fishing in lakes and streams. It is prohibited because it kills all living things in the water and fish caught in this way are dangerous because they cause poisoning in humans (Tanker et al., 1998; Baytop, 1999; Ateş, 2001). E. rigida is a one or two year old plant with bluish-green colour. It has a woody storage root and a narrow spear-like stem with dense leaves. The body has simple, thick and fleshy leaves facing one another, and umbrella-shaped flowers. The fruit of the plant has a round capsule-like structure with three seeds. Its seeds are light gray or white in colour. Flowering time is between March and August and can develop at altitudes varying from sea level to 2000 m. It is seen in the cities of Tekirdağ, Canakkale, İstanbul, Amasya, Tokat, Manisa, Aydın, İzmir, Kayseri, Niğde and Antalya in Turkey (Baytop, 1998). Many Euphorbia species have been used all over the world and in Turkish culture by our people since old times for medical purposes such as laxatives, the removal of warts, the treatment of aphthae, bronchitis, cold, cough, emphysema, measles, peptic ulcer, haemorrhoids, nausea, acute mastitis, diuretics and enhancing milk secretion (Barla et al., 2007; Shi et al., 2008; Kırbağ et al. 2013; Erdoğan et al., 2012; Huang et al., 2012; Özbilgin and Çitoğlu-Saltan, 2012; Ghareeb et al. 2018; Ghosh et al., 2019: Kemboi et al., 2020). It is also known that it has been used for centuries as a colouring material (Tiryakioğlu, 2004) and as a biopesticide to preserve food stocks (Şahin et al. 2006). With antimicrobial activity studies conducted with some Euphorbia genus, it has been observed that herbal extracts of Euphorbia species have different levels of antimicrobial activity against Gr (+), Gr (-) bacteria and fungal infectious agents (Özbilgin and Çitoğlu-Saltan, 2012). Plants belonging to the Euphorbiaceae family are

rich in bioactive compounds such as tiglian, ingenan and dafnan diterpenoids which have phenolic, flavoniod, especially terpenoid and steroid characteristics responsible for antioxidant effects (Tiryakioğlu, 2004; Barla et al., 2007). The same compounds are responsible for the bactericidal effects and toxic and irritating properties observed in studies with Euphorbia species (Barla et al., 2007; Shi et al., 2008; Wu et. al., 2009).

Today, resistance develops in pathogenic microorganisms and agricultural pests against many natural and synthetic compounds. For this reason, the new natural compounds obtained from plants have been tested in in vitro and in vivo conditions with biological effect tests and preferred as a biopesticide, natural antioxidant and antimicrobial source, and the interest in their applicability to humans has increased (Dülger et al., 1998; Turan-Zitouni et al., 2005a, b; Kırbağ and Zengin, 2006; Aksoy et al., 2008; Tanış et al., 2010). One of the biological tests, Brine-Shrimp test (Artemia salina larvae) is widely used as a fast and simple method in the determination of cytotoxicity of samples whose biological activities are investigated (Choudhary and Thomsen, 2001).

By using our natural resources, chemical raw materials can be obtained more cheaply and easily and an important economic contribution can be made to our country. For this purpose, the safe dose of Euphorbia rigida plant extract from the Euphorbiacea family, which has the capacity to be used as a biopesticide (Civelek and Weintraub, 2004), antimicrobial (Başaran et al., 1996; Özbilgin and Çitoğlu-Saltan, 2012) and antioxidant (Barla et al., 2007) and which is widely grown in Muğla province was tested by means of Brine shrimp cytotoxicity test (Brine shrimp lethality assay).

2 Materials and Methods

2-1 Collection of the plants and their extraction

The aerial parts of Euphorbia rigida (Bieb.) in the flowering period were collected from Muğla Sıtkı Koçman Üniversity campus (GPS:37°09'40,1"N 28°22'34"E) in Muğla at Turkey. The taxanomic identification of plant materials was confirmed and deposited in the herbarium by voucher specimen Dr. Olcay Ceylan at the Department of Biology a Muğla Sıtkı Koçman University (Herbarium number: 0388). The samples were air-dried at room temperature and protected from direct sunlight. Seventyfive (75 g) grams of dried and powdered aerial parts of E. rigida were extracted with 2.5 L boiling water for 60 min. Decoction (aqueous phase) was filtered with a 2.5 µm filter paper (Whatman No. 42) to remove suspended particles and the extract was kept at least 3 days at -20°C and later lyophilized to obtained crude (6.72 g) extract which was stored at -20°C (Özbek et al., 2002).

2-2 Preparation of Artemia salina larvae

The SERA brand (Sera North America, Inc. Montgomeryville, U.S.A.) Artemia salina eggs (cysts) purchased from a company that sells aquarium materials were weighed to be 2 grams and then sprinkled into a 5-liter plastic, transparent, open-mouthed tank containing 2 litres of artificial sea water. The artificial sea water in the tank is continuously aerated by a double outlet air motor using double hoses. In addition, the water temperature in the tank was heated to a constant 28°C by a thermostat. The tank was left in the light for approximately 48 hours next to a desktop light source, and Artemia salina larvae (nauplii) were waited to hatch from the eggs. Experimental setup is shown in Figure (1), the image of Artemia salina eggs is shown in Figure (2), and the hatched Artemia salina larvae are shown in Figures (3 a *and* b).

Fig. 1: Experimental Setup

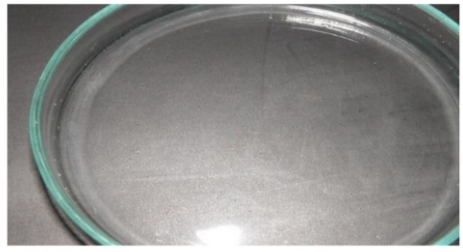

Fig 2: Artemia salina eggs

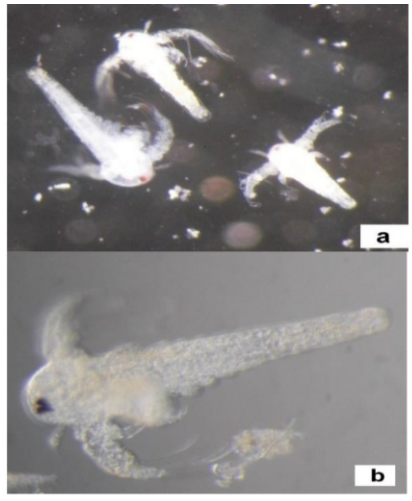

Fig. 3: Artemia salina larvae emerged from eggs (a), a single larva (b)

2-3 Brine shrimp cytotoxicity test (Brine shrimp lethality assay)

Artemia salina larvae are one of the toxicity test organisms used to determine the LC50 level. Diluted solutions of 10, 20, 30, 40 and 50 ppm prepared from the dry extract obtained from the aqueous extract of E. rigida plant, sterile artificial sea water prepared with distilled water for control purposes (35 g non-iodized rock salt, 1000 ml sterile distilled water) and 20, 100 and 200 ppm solutions of Elandor® (İmidacloprid) used as insecticide (the recommended dose in agricultural practice is 200 ppm, Öncüer, 2004) were used to test the cytotoxic effect by means of Brine Shrimp method. As a result of the study, the LC50 value was calculated (Table 1) and the toxicity levels (Brayn et al., 1997) (Table 2) were determined. The study was conducted according to Sowemimoa et al., 2007.

2-4 Cytotoxic effect determination

Stock solutions of 100 ppm, 200 ppm, 300 ppm, 400 ppm and 500 ppm were prepared from E. rigida plant extract

with distilled water. 500 µl of each of the stock solutions were taken and put into glass test tubes adjusted to a volume of 5 ml. The top of the test tubes are completed to 5 ml with sterile artificial sea water. Thus, diluted solutions of 10 ppm, 20 ppm, 30 ppm, 40 ppm and 50 ppm concentrations where the applications would be conducted were obtained. Elandor stock solutions were diluted in a similar way, and final concentrations of 20, 100 and 200 ppm where the applications would be conducted were obtained.

Artemia salina larvae migrate in the water after hatching towards the area where the light is intense (Choudhary and Thomsen, 2001). Thus, the larvae taken from the part where the larvae were dense with the help of a micropipette together with approximately 10 µl of water were transferred into a petri dish under stereomicroscope and 30 larvae were counted. 30 living organisms were transferred to into tubes (Control) with 5 ml sterile artificial sea water, glass tubes containing E. rigida plant extract in concentrations of 10 ppm, 20 ppm, 30 ppm, 40 ppm and 50 ppm and glass tubes containing 20, 100 and 200 ppm solutions of Elandor used as insecticide. The study was carried out in 3 parallels. At the end of 24 hours under light, the numbers of live and dead larvae (defined as dead according to their immobility) were counted with the help of a magnifying glass. The obtained results were transferred to the EPA (The U. S. Environmental Protection Agency, Cincinnati, Ohio, U.S.A.) Probit Analysis Program (Version 1.5) and the LC50 value and 95% confidence lower and upper limits were calculated (EPA, 2021). LC50 values obtained were interpreted according to Brayn et al., 1997.

Table 1 : Approximate LC / EC values and confidence limits for E. rigida and Elandor according to EPA Probit Analysis Program (Version 1.5)

	Euphorbia rigida			**Elandor® (İmidacloprid)**		
LC/EC	Concentration Exposed	95% Confidence Limits µg/ml (ppm)		Concentration Exposed	95% Confidence Limits µg/ml (ppm)	
	µg/ml (ppm)	Lowest	Highest	µg/ml (ppm)	Lowest	Highest
LC/EC 1.00	3.772	0.00	12.147	47.895	0.002	90.700
LC/EC 5.00	8.352	0.00	18.874	71.870	0.061	114.329
LC/EC 10.00	12.759	0.00	24.179	89.232	0.425	130.414
LC/EC 15.00	16.983	0.05	28.964	103.263	1.558	143.648
LC/EC 50.00	**56.888**	**36.146**	**1831.913**	**191.437**	**131.752**	**621.028**
LC/EC 85.00	190.554	85.077	348011456.000	354.902	236.843	126261.281
LC/EC 90.00	253.645	99.947	6433705472.000	410.708	258.595	467149.125
LC/EC 95.00	387.489	126.263	%4871515013l2.0	509.926	293.040	3262383.500
LC/EC 99.00	857.88	194.139	%164366989.132E	765.178	367.492	125955424.0

Table 2 : Reference values used to evaluate the degree of toxicity (Brayn et al., 1997).

Toxicity Degree	**LC_{50} Limits**
Highly toxic	< 10 µg/ml
Toxic	10-100 µg/ ml
Harmful	100-1000 µg/ ml
Not toxic	> 1000 µg/ ml

3 Results and Discussion

According to the Brine-shrimp general toxicity test result, the LC50 value of the extract obtained from E. rigida Bieb. with water was found to be 56.89 ppm, the 95% confidence lower limit was found to be 36.15 ppm and the upper limit was found to be 1831.91 ppm (Table 1), and it was concluded that the E. rigida Bieb. plant extract was toxic according to the toxicity reference values (Table 2., Brayn et al., 1997). In addition, the LC50 (191.437 ppm) value and 95% confidence lower and upper limits (Table 1) of Elandor (Imidacloprid) used as a chemical pesticide in agricultural control are considered to be in the pest class according to the toxicity reference values (Table 2., Brayn et al., 1997) and it was concluded that plant extract of E. rigida Bieb. is more toxic and dangerous. The results we have obtained in our study are consistent with the results of many cytotoxicity studies conducted with various Euphorbia species. LC50 value of extracts obtained from all tissues of E. hirta except for flowers were found by Brine shrimp lethality test method (LC50 = 1000 ug / ml) (Huang et al., 2012). Brine shrimp lethality test was used to investigate the cytotoxicity of Euphorbia hirta. The study concluded that the LC50 of ethyl acetate and acetone decoction of plant parts were 71.15 and 92.15 µg/ml, respectively (Ghosh et al., 2019). The E. hirta extract also showed selective anticancer activity at a concentration of 100 µg/mL (Alam et al., 2016). E. microsciadia and E. szovitsii indicated the highest anti-breast cancer activities on cancer cell lines and the lowest IC50 was 59.52 µg/mL which was found for E. szovitsii against MCF-7 cell line (Asadi-Samani et al., 2019) The LD50 values of 17-acetoxyjolkinolide B and 13-hexadecanoyloxy-12-deoxyphorbol obtained from the dry roots of E. fischeriana and lathyrane diterpenoids isolated from E. nivulia were reported to have approximately the same and significant cytotoxic effect against the Colo 205, MT2 and CEM cell lines (Shi et al., 2008). IC50 values of the cytotoxic effect of compounds obtained from the dry roots of E. fischeriana against Ramos B cells are approximately 0.023 and 0.0051 µg / ml, respectively (Wang et al., 2006). The daphnane and tigliane diterpenoids isolated from the latex of E. poisonii showed a selective and potent cytotoxic effect on human kidney carcinoma (A-498) cell lines. This effect was found to be 10 000 times greater than adriamycin (Fatope et al., 1996). While the ED50 values of the compounds obtained from E. poisonii were between 2 and 4 µg / ml, they showed a weak non-selective cytotoxic effect against A-549, MCF-7, HT, A-498, PC-3, and PACA-2 cell lines. On the other hand, when its ED50 value is 15 µg / ml, it has weak but selective cytotoxic effects against prostate adinocarcinoma (PC-3) (Wang et al., 2006; Shi et al., 2008).

Cytotoxic activities of extracts obtained from four species belonging to the Euphorbia genus (E. fischeriana, E. tirucalli, E. humifusa and E. antiquorum) on the development of human liver carcinoma cells (BEL-7402) and human lung cancer cells (A-549) were investigated with the inhibition test method in in vitro conditions. Extracts are considered effective at the lowest IC50 = 30 µg / ml dose. Chloroform extracts obtained from E. tirucalli and E. antiquorum showed strong cytotoxic activity in both human cancer cell lines. Chloroform and ethylacetate extracts obtained from E. fischeriana showed significant cytotoxic activity only on human lung cancer cell (A-549) (Wang et al., 2006).

Diterpenoid compounds in E. paralias extracts have high molluscoidal activity on Biomphalaria alexandrina. The antifeedant activity of E. paralias was tested against Spodoptera littoralis third stage larvae with the disc leaf method, a traditional test. Some compounds (at a dose of

1000 mg / ml) showed an antifeedant activity against insects by an average of 66.8% and 45.8% (Abdelgalil et al., 2002; Shi et al., 2008). Strong molluscoidal activity of the aqueous extracts of E. pulcherima and E. hirta plants and partially purified latex against Lymnaea acuminata (LC50 = 40% and 80%) was observed (Shi et al., 2008; Özbilgin and Çitoğlu-Saltan, 2012; Huang et al., 2012). E. hirta Linn latex powder was evaluated against the freshwater snails Lymnaea (Radix) acuminata and Indoplanorbis exustus in pond (Alam et al., 2016; Ghosh et al., 2019).

The petroleum ether fraction of E. hirta showed strong larvicidal activity in the third stage larvae of Anopheles stephensi, which is known as the malaria vector in cities. The flavonol glycoside afzelin, quercitin and myricitin isolated from E. hirta at different concentrations showed an inhibition effect on the proliferation (Anti-malarial) of Plasmodium falcifarum (Wang et al., 2006; Huang et al., 2012; Özbilgin and Çitoğlu-Saltan, 2012; Alam et al., 2016; Ghosh et al., 2019).

It is reported that latex belonging to Euphorbia species is used against wireworms in corn and soybean cultivation and also for nematode control in tomatoes, potatoes and peppers. It is reported that the species belonging to Cuphea genus from the Euphorbiaceae family and the plant extract called Euphorbia lagascae are effective against corn worm, wireworm and grayworm in tomato, potato, bean and clover; it has also been reported that the same extracts can be an alternative to methyl bromide applications with an effective rate of 97% on nematodes that damage potato plants (Civelek and Weintraub, 2004). E. orientalis L. was found containing bioactive compounds that have essential antibacterial and antioxidant activities. Therefore, the possibility of using Euphorbia species and E. rigida extract as an antiseptic for sterilization or disinfection of large and inanimate surfaces can be explored (Avcı et al. 2013; Metin and Bürün, 2021).

According to the brine-shrimp general toxicity test result, the LC50 value of the extract obtained from Euphorbia rigida Bieb. with water is 56.89 ppm, which supports its usability as a biopesticide in agricultural control as an alternative to chemical pesticides such as Elandor, which we used for comparison in the same study. However, studies on the systematic toxicity and safety assessment of Euphorbia species are very few. In the studies conducted, only the organs that it affects (targets) toxically and their side effects have been emphasized (Huang et al., 2012).

4 Conclusion

Antibacterial, antifungal and antiviral properties of Euphorbia extracts are well known, so it could mean that they can be used as additives or a disinfectant for inanimate surfaces in the pharmaceutics industry. By investigating the chemical contents of various extracts obtained from E. rigida plant, determining the optimum conditions and identifying and isolating the compounds responsible for the activity in in vitro and in vivo conditions as a new and alternative cytotoxicity (anticancer) and biopesticide agent, it has been shown that it can be used as a raw material in pharmaceutical and industrial (cleaning and sterilization) activities.

According to the results of this research, we can suggest that the extract obtained from E. rigida plant with water up to 57 ppm can be used as an alternative to chemicals used as biopesticide. When extract of E. rigida is used, great care should be taken while using it because it can cause damage on cells and chromosomes (Metin and Bürün, 2021). Hence, through more detailed and comprehensive studies, its usability for medical and biopesticide purposes should be investigated.

Disclosure statement

No potential conflict of interest was reported by the authors.

References

[1] JAbdelgalil SAM, El-Aswad AF, Nakatani M., (2002). Molluscicidal and anti-feedant activities of diterpenes from Euphorbia paralias L. Pest Manage. Sci. 58: 479-482.

[2] Abay, E., (2006). Bazı Bitki Ekstraktlarının Antibakteriyel Etkilerinin Disk Difüzyon Yöntemiyle Araştırılması. Yüksek Lisans Tezi, Kafkas Üniversitesi, Kars. 34s.

[3] Aksoy, A., Albayrak, S., Sagdic O., (2008). Türkiye'de Yetişen Endemik Salvia halophila'nın Antimikrobiyal ve Antioksidan Aktivitesinin Belirlenmesi. Türkiye 10. Gıda Kongresi, 21-23 Mayıs 2008, Erzurum.

[4] Alam A.A, Tarannum K, Parwez A. Md, Gupta Ravi Shankar G.R, Mukhtar A, Laxmi N.N., (2016). A review on pharmacological and chemical documentation of Euphorbia hirta Linn (Asthama Herb). An Official Journal of NMC, Birgunj, Nepal, Volume (1), Issue (1). 31-38.

[5] Arıkan, S., (1992). Bazı Tohumlu Bitki Ekstrelerinin Çeşitli Mikroorganizmalar Üzerindeki Antibakteriyel Etkileri, Kükem Der. 15(2): 39-47.

[6]Asadi-Samani, M., Rafieian-Kopaei, M., Lorigooini, Z., Shirzad, H., (2019). A screening of anti-breast cancer effects and antioxidant activity of twenty medicinal plants gathered from Chaharmahal va Bakhtyari province, Iran. Journal of Pharmacy & Pharmacognosy Research, 7(3), 213-222,

[7] Ateş, F., (2001). Euphorbia rigida'nın Sabit Yatak Reaktörde Katalitik Pirolizi. Doktora Tezi, Anadolu Üniversitesi, Eskişehir.

[8] Avcı G.A, Avcı E, Köse D.A, Akçal İ.H., (2013). Investigation of applicability instead of chemical disinfectants of Euphorbia orientalis L. extracts. Hacettepe J. Biol. & Chem., 41(2), 151-157

[9] Barla, A., Öztürk, M., Kültür, Ş., Öksüz, S., (2007). Screening of Antioxidant Activitiy of Three Euphorbia Species from Turkey. Fitoterapia 78, 423-428.

[10] Başaran, A.A., Yu, T-W., Plewa, M.J. Anderson, D., (1996). An Investigation of some Turkish Herbal Medicines in Salmonella thyphimurium and in the Comet assay in human lymphocytes, Teratogenesis, Carcinogenesis and Mutagenesis, 16 (2), 125-138.

[11] Baytop, A., (1998). Tıbbi bitkiler hakkında Anadolu halkı arasındaki bilgilerin kaynakları. New strends and methods in natural products research, XII th International Symposium on Plant Originated Crude Drugs, 20-22 May 1998, Ankara.

[12] Baytop, A., (1999), Türkiye de bitkiler ile tedavi: Geçmişte ve bugün. 2. baskı, Nobel Tıp Kitabevi Yayınları, İstanbul, 18-56.

[13] Baytop, A., (2000), Anadolu dağlarında 50 yıl, Bir bitki avcısının gözlemleri. Nobel Tıp Kitabevi Yayınları, İstanbul, 113-118. Brayn, B., Timothy, M., Tore, S., (1997). General and Applied Toxicology, 2nd. Edition,1, 52.

[14] Choudhary, I.M., Thomsen, W.J., (2001). Bioassay Techniques For Drug Development, Harwood Academic Publishers, 8-10.

[15] Civelek H.S, Weintraub P.G., (2004). Effects of two plant extracts on larval leafminer Liriomyza trifolii (Diptera: Agromyzidae)

[16] Çalışkan, T., Hatipoğlu, R., Kırıcı, S., (2019). Production of Plant Secondary Metabolites from Cell and Organ Cultures under In vitro Conditions Turkish Journal of Agriculture - Food Science and Technology, 7(7): 971-980.

[17] Çelik, E., Çelik, G.Y., (2007). Bitki Uçucu Yağlarının Antimikrobiyal Özellikleri. Orlab On-Line Mikr. Der.,5(2):1-6

[18] Dülger, B., Gücin, F., Aslan, A., (1998). Cetraria islandica (L.) Ach. Likeninin Antimikrobiyal Aktivitesi. Tr. J. of Biology. 22; 111-118.

[19] EPA,.(2021).http://www.epa.gov/pesticides (search.epa.gov/epasearch/ Brine-shrimp).

[20] Erdoğan, N., Büyükkartal, H. N., Çölgeçen, H., Karadeniz, A., (2012). Sertavul Geçidi ve Mut (Mersin) Çevresinde Yayılış Gösteren Bazı Euphorbia L. Taksonlarının Anatomik Yönden İncelenmesi. Mehmet Akif Ersoy Üniversitesi Fen Bilimleri Enstitüsü Dergisi 3 (1): 22-31.

[21] Fatope M.O., Zeng L., Ohayaga J.E., Shi G., McLaughlin J.L., (1996). Selectively cytotoxic diterpenes from Euphorbia poisonii, J Med Chem 39, 1005-1008.

[22] Ghareeb A.T., El-Toumy S.A., El-Gendy1 H., Haggag E.G., (2018). Secondary metabolites and hepatoprotective activity of Euphorbia retusa. JAPR, 2 (4), 283-291.

[23] Ghosh P., Ghosh C., Das S., Das C., Mandal S., Chatterjee, S., (2019). Botanical description, phytochemical constituents and pharmacological properties of Euphorbia hirta Linn. A Review. www.ijhsr.org, Vol.9; Issue: 3

[24] Huang, L., Chen, S., Yang, M., (2012). Euphorbia hirta (Feiyangcao): A review on its ethnopharmacology, phytochemistry (Feiyangcao): A review on its ethnopharmacology, phytochemistry and pharmacology. J. of Med. Plants Res.,Vol. 6(39): 5176-5185

[25] Kemboi, D., Peter, X., Langat, M., Tembu, J., (2020). A Review of the Ethnomedicinal Uses, Biological Activities, and Triterpenoids of Euphorbia Species. Molecules, 25, 4019. doi:10.3390/molecules25174019

[26] Kırbağ, S., Zengin, F., (2006). Elazığ Yöresindeki Bazı Tıbbi Bitkilerin Antimikrobiyal Aktiviteleri. Yüzüncü Yıl Ünv. Ziraat Fakültesi, Tarım Bilimleri Dergisi, 16(2), 77-80

[27] Kırbağ S., Erecevit P., Zengin F., Guvenc A.N., (2013). Antimicrobal activities of Euphorbia species. Afr J Tradit Complement Altern Med. 10(5):305-309 http://dx.doi.org/10.4314/ajtcam.v10i5.13

[28] Koca, İ., Karadeniz, B., (2003). Serbest Radikal Oluşum Mekanizmaları ve Vücuttaki Antioksidan Savunma Sistemleri. Ankara Üniversitesi, Ziraat Fak. Gıda Müh. Der., S:32-37 www.gidamo.org.tr (15.01.2020).

[29] Metin, M., Bürün, B., (2021). Investigation of the Cytotoxic and Genotoxic Effects of the Euphorbia rigida Bieb. Extract. Caryologia, DOI:10.13128/caryologia-1029.

[30] Özbek, H., Özgökçe, F., Ceylan, E., Taş, A., Tunçtürk, M., (2002). Secale cerealeL. (Çavdar) Meyvesi Dekoksiyon Ekstresinin Sağlıklı ve Diyabetli Farelerde Hipoglisemik Etkisinin Araştırılması. Van Tıp Dergisi 9(3):73-77.

[31] Özbilgin, S., Çitoğlu-Saltan, G., (2012) Uses some Euphorbia Species in Traditional Medicine in Turkey and Their Biological Activities. Turk J. Pharm. Sci. 9(2), 241-256.

[32] Özmen, A., Sümer, Ş., (2004). Cytogenetic Effects of Kernel Extracts from Melia azedarach L. Caryologia, Vol.57, No. 3:290-293.

[33] Sarışen, Ö., Çalıskan, D., (2005). Fitoterapi: Bitkilerle Tedaviye Dikkat, Sted, 14(8), 182-187.

[34] Shi, Q-W., Su, X-H., Kiyota, H., (2008). Chemical and Pharmacological Research of the Plants in Genus Euphorbia. Chem. Rev. 108, 4295–4327. American Chemical Society Published on Web 09/25/2008.

[35] Sowemimoa, A. A., Fakoya, F. A., Awopetu, I., Omobuwajo, O. R., Adesanya, S.A., (2007). Toxicity and Mutagenic Activity of Some Selected Nigerian Plants, Journal of Ethnopharmacology, 113, 427–432.

[36] Şahin A., Erçel S., Akşit H., Damar R., Dulkadir K., Demirtas İ., (2006). Sütleğen (Euphorbia allepica L.) bitkisinin sekonder metabolitlerinin saflaştırılması, karakterizasyonu ve bazı biyolojik aktivitelerinin incelenmesi, Türkiye Kayseri: XX. Kimya Kongresi, Erciyes Üniversitesi.

[37] Tanış, H., Karcıoğlu, L., Dıraz, E., Aygan, A., (2010). Kahramanmaraş Bölgesinde Yetişen Işgın (Rheum ribes L.)'ın Antibakteriyal Aktivitesinin Belirlenmesi. KSÜ Doğa Bil. Derg., 13(2).

[38] Tanker, N., Koyuncu, M., Çoşkun, M., (1998). Farmasötik Botanik. Ankara Ünv., Ecz. Fak. Yayınları, Ders Kitapları No: 78, S. 169-170.

[38] Tiryakioğlu, B., (2004). Euphorbia seguieriana Bitkisinden Hazırlanan Özütlerin Antibakteriyel Etkilerinin İncelenmesi. Yüksek Lisans Tezi, Onsekiz Mart Üniversitesi, Çanakkale. 98s.

[39] Turan-Zitouni, G., Özdemir, A., Güven, K., (2005a). "Synthesis of some 1-[(N,N-disubstitutedthiocarbamoylthio)acetyl]-3-(2-thienyl)-5-aryl-2- pyrazoline derivatives and investıgation of their antibacterial and antifungal activities", Archiv der Pharmazie-Pharmaceutical and Medicinal Chemistry 338(2-3), 96-104.

[39] Turan-Zitouni, G., Kaplancıklı, Z. A., Yıldız, M. T., Chevallet, P., Kaya, D., (2005b). "Synthesis and antimicrobial activity of 4-phenyl/cyclohexyl-5-(1-phenoxyethyl)-3-[N-(2 thiazolyl)acetamido] thio - 4h-1,2,4 -triazole derivatives", Eur. J. Med. Chem. 40, 607-613.

[40] Wang, X., Liu, L., Zhu, R., Kang, T., Tong, L., Xie, H., Wang H., (2006). Cytotoxic activities of some selected medicinal plants of the genus Euphorbia. Journal of Medicinal Plants Research Vol. 5(31), pp. 6766-6769.

[41] Wu, Q.C., Tang, Y.P., Ding, A.W., You, F.Q., Zhang, L., Duan A.D., (2009). 13C-NMR data of three important diterpenes isolated from Euphorbia species. Molecules 14(11):4454-75.

Keratin Protein Based Bioplastic Mixed With Microcrystalin Cellulose

Rabia YİGEN, Ayşe ONGUN YÜCE , Adana Bahtiyar Vahabzade Social Sciences High School, Adana, Turkey

rabia.yigen1714@gmail.com , ayseongunyuce@gmail.com

ARTICLE INFO

This study is a part of a PhD thesis.

Winner of Gold Medal in IMSEF 2020, Turkey, Izmir and was awarded by Ariaian Young Innovative Minds Institute , AYIMI

http://www.ayimi.org , info@ayimi.org

ABSTRACT

In this study , keratin protein (KP) consisting of cystine amino acids was obtained by precipitation of human hair in an alkaline environment. The obtained protein was mixed with microcrystalline cellulose (filler) (MS), plasticizer at appropriate proportions and temperature until it reached gel consistency. According to the results obtained, it is seen that the highest degradation is achieved in sea water, whereas KP-based bioplastics do not have a very long-term resistance to dissolution in soil and sea water under normal conditions, dissolve in a short time and do not cause pollution in the environment. Therefore, KP bioplastics can be used in industrial applications such as the food, packaging, and agriculture industry.

Key Words : *MS, KP , bioplastic, biodegradation, alkaline environment*

1 Introduction

More than 300 million tons of petroleum-based or gas-based polymers are produced annually worldwide, and mostly in almost all areas of daily life (agricultural, packaging, construction, transportation, electrical and electronic equipment, etc.) and the processing industry (chemical, food, aerospace, pharmaceuticals, etc.) are used in the production of non-biodegradable plastics for a wide variety of applications [1]. For environmental pollution caused by the wide application of petroleum-based plastics, the production of biodegradable materials based on naturally occurring resources including proteins, polysaccharides, lignin, etc. has become a new research topic in materials science and engineering. [2-4] Bio-based plastics represent a broad spectrum of materials that can be synthesized by living organisms (i.e. naturally produced bio-based polymers such as proteins or polysaccharides) or that can be derived from renewable sources in their monomer forms that require chemical change to convert to a polymer (e.g. PLA from lactic acid). Among these, protein is the most promising bio-based sources for bioplastics, as protein-based materials tend to form three-dimensional macromolecular networks stabilized and reinforced by hydrogen bonds, hydrophobic interactions, and disulfide bonds [5]. Among them, the keratin protein has a large structure that provides an outer covering in the form of hairs, wool, feather horns and nails in most mammals, birds, and reptiles. Biodegradation is an organic, biodegradable polymer resulting from the cross-linking of long, strong covalent bonds in its structure [6]. Typically, the production of protein-based bioplastics involves chemical, thermal or pressure-induced protein denaturation as a first step. Due to the diversity and unique structures in the assembly of protein networks, a wide variety of biodegradable materials can be produced and various functional properties can be given [7]. However, protein hydrolysates are prepared to increase their solubility, nutritional supplementation, and their use for functional enhancement [8]. One of the most interesting potential uses of these products is the production of bioplastics that solve the problem of environmental pollution. However, a variety of different protein concentrates have been used to produce bioplastics [9-11]. It has also been suggested to use mixtures of these proteins with synthetic additives to achieve good mechanical properties for biodegradable plastics (for example, for the production of food packaging) [12-15]. Before heat treatment during the production of a bioplastic, it is necessary to obtain a pulp, which is a mixture of protein concentrate and plasticizer [16]. The role of the plasticizer is to reduce the glass transition temperature (Tg) and provide mobility to polymeric chains, reducing electrostatic and hydrophobic interactions [17] and therefore a polar and low molecular weight plasticizer such as glycerol (GL) is used.

In the present study, keratin protein (KP), which is composed of cysteine amino acids, was obtained by precipitation of human hair in an alkaline environment. The obtained protein was mixed with microcrystalline cellulose (filler) (MS), plasticizer at appropriate proportions and temperature until it reached gel consistency. Then, the viscous mixture was poured into molds and freezing was achieved. The biodegradable plastic formulation may contain a lubricant to easily remove the bioplastic from the mold. Protein and plasticizer ratios are pre-optimized for the production of keratin-based bioplastics. Biodegradability of the obtained bioplastics was tested in soil and sea water. In addition, the water absorption percentage of the bioplastic was also determined.

2 Materials and Methods

Natural human hair that has not undergone any chemical treatment such as dyeing and conditioning was provided from the hairdresser. Analytical grade sodium hydroxide, glycerin, microcrystalline cellulose, hydrochloric acid and nano titanium dioxide (N-TiO2) were purchased from Sigma Aldrich (St. Louis, USA). Natural habitat soil and sea water were used for biodegradability testing of KP-based bioplastics.

After cleaning 50 g of human hair with ethanol and distilled water, the cleaned, dried and mixed hair was incubated in 1 L sodium hydroxide (1 N) solution at 50 ° C for five hours with continuous stirring, After that, the solution was washed with distilled water and filter paper. filtered with. The resulting keratin protein was then allowed to dry at room temperature for bioplastic synthesis. (Fig.1).

(a)

(b)

Fig. 1: KP solution obtained (a) and infiltration (b).

PVA powder (15 g) was dissolved in 100 ml of water and stirred at 80 ° C for one hour. First, KP was mixed with 10% glycerol, cellulose (2%) and 30% PVA solution at 60 ° C. The mixture was then poured into silicone molds and oven dried at 50 ° C for 24 hours. Later, biodegradation time in soil and sea water, solubility in different solutions and water absorption were saved (Fig. 2).

Fig. 2: Production and molding of KP based bioplastics

The same amounts of mixture (3 g) were placed 15 cm below the bioplastic soil level in four locations for the degradation analysis of the synthesized bioplastics in the open air surrounding soil. After 15 days the mass loss change of the bioplastics was measured. Likewise, equal amounts (3 g) of bioplastics were added to four beakers containing 50 ml of sea water and kept for 15, 30, 45 days. The extracted bioplastics were freed in the oven (50 ° C), and the mass loss was calculated according to equation (1) by measuring the initial (Kb) and subsequent masses (Ks) of each. The degradation time of bioplastics for sea water and soil was tried to be determined by plotting the weight loss versus time .

$$\text{Weight loss} = Kb\text{-}Ks / Kb \quad (1)$$

3 Results and Discussion

Biodegradable plastics was prepared by taking glycerin, microcrystalline cellulose and KP, NaOH, HCl in appropriate proportions . Biodegradability, solubility in different solutions and water absorption of the obtained bioplastics under room conditions (soil, sea water) were tested.

3.1 Biodegradability Tests

The percentage of weight loss of the obtained bioplastics in room conditions (soil and sea water) versus time is shown in Figures (3 a and b) , respectively. By comparison between these two figures, it is seen that the biodegradation of bioplastics is higher in sea water (78%) than in soil (59%). This situation is related to the increasing or decreasing in the degradation of the bioplastic as a result of the change of seawater flora (temperature, humidity and microorganisms etc) versus time.

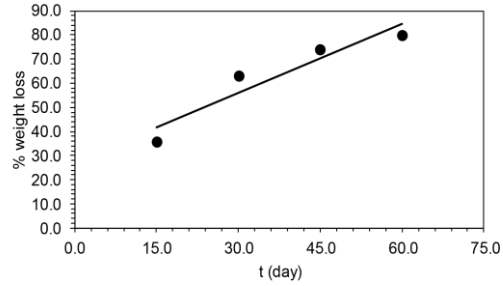

(a)

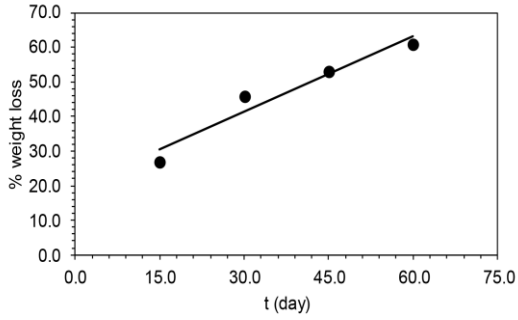

(b)

Fig. 3: Weight loss vs. time of the degradation of KP-based bioplastics in soil (a) and seawater (b), respectively, under room conditions

3.2 Solubility Test

The solubilities of the KP-based bioplastic in different solutions, concentrated acid (a), concentrated base (b) and pure ethanol (c), are shown in Figure (4).

(a) (b) (c)

Fig. 4: Dissolution of KP-based bioplastics in different solutions

It is seen that bioplastics dissolve rapidly in the acid solution, where they form different colors while dissolving in solutions. Therefore, it is thought that KP-based bioplastic may be used in the packaging industry.

4 Conclusion and Suggestions

KP based bioplastics were obtained using analytical grade dilute HCl, NaOH, glycerine, microcrystalline cellulose and N-TiO2. The decomposition of the obtained plastics to their biological parts was found to be 59% and 78%, respectively, in soil and sea water. According to the results obtained, it is seen that the highest degradation is achieved in sea water, whereas KP-based bioplastics do not

have a very long-term resistance to dissolution in soil and sea water under normal conditions, dissolve in a short time without pollution in the environment. Therefore, KP bioplastics can be used in industrial applications such as the food, packaging, and agriculture industry.

Acknowledgements

Author is highly thankful to Prof. Dr. Gülfeza KARDAŞ for valuable contributions and Çukurova University Faculty of Arts and Sciences Department of Chemistry Physical Chemistry Research Laboratory for supporting this work.

References

[1] Halden, R.U., (2010). Plastics and health risks. Annual Review of Public Health 31, 179–194.

[2] Tian, H., Yan, J., Rajulu, A.V., Xiang, A., Luo, X., (2017). Fabrication and properties of polyvinyl alcohol/starch blend films: effect of composition and humidity, International Journal of Biological Macromolecules, 96, 518–523.

[3] Chen, Q., Gao, K., Peng, C., Xie, H., Zhao, Z.K., Bao, M., (2015). Preparation of lignin/glycerolbased bis(cyclic carbonate) for the synthesis of polyurethanes, Green Chemistry, 17, 4546–4551.

[4] Muthulakshmi L., Rajini, N., Nellaiah, H., Kathiresan, T., Jawaid, M., Rajulu, A.V., (2017). Preparation and properties of cellulose nanocomposite films with in situ generale copper nanoparticles using Terminalia catappa leaf extract, International Journal of Biological Macromolecules, 95, 1064–1071.

[5] Thomas, S., Durand, D., Chassenieux, C., Jyotishkumar, P., (2013). Handbook ofBiopolymer-base Materials: From Blends and Composites to Gels and Complex Networks. Wiley-VCH, Verlag GmbH, Germany.

[6] Kumawat, T.K., Sharma, A., Sharma, V., Chandra, S., 2018. Keratin Waste: The Biodegradable Polymers. Keratin. IntechOpen.

[7] Verbeek, C.J.R., van den Berg, L.E., (2010). Extrusion processing and properties of protein-based thermoplastics. Macromolecular Materials and Engineering, 295, 10–21.

[8] Guo, X.F., Zhang, J.J., Ma, Y.X., Tian, S.J., (2013). Optimization of limited hydrolysis ofproteins in rice residue and characterization of the functional properties of the products. Journal of Food Processing. 37, 245–253.

[9] Gomez-Martinez, D., Partal, P., Martinez, I., Gallegos, C., (2013). Gluten-basedbioplastics with modified controlled-release and hydrophilic properties. Industrial Crops and Products. 43, 704–710.

[10] Jerez, A., Partal, P., Martinez, I., Gallegos, C., Guerrero, A., (2007). Protein-based bioplastics: effect of thermo-mechanical processing. Rheologica Acta, 46, 711–720.

[11] Kim, S., (2008). Processing and properties of gluten/zein composite. Bioresour.Technol. 99, 2032–2036.

[12] Min, Z., Song, Y., Zheng, Q., (2008). Influence of reducing agents on properties ofthermo-molded wheat gluten bioplastics, Journal of Cereal Science, 48, 794–799.

[13] Pickering, K.L., Verbeek, C.J.R., Viljoen, C., (2012). The effect of aqueous on the processing, structure and properties of CGM. Journal of Polymers and the Environment. 20, 335–343.

FRICTION OSCILLATOR

Sahar Semsarha ,Farzanegan2 high school, Tehran/ Iran, sahar.sems@gmail.com

ARTICLE INFO

Winner of Silver Medal , IMSEF 2020, Turkey

Participated in O-IYPT 2020

Accepted in country selection by Ariaian Young Innovative Minds Institute , AYIMI

http://www.ayimi.org ,info@ayimi.org

ABSTRACT

This essay is about oscillation of a massive object place on the rotating cylinders' witch rotate in opposite directions. The place and frequency of the massive object have been investigated. Although a simulation has been presented and affective parameters like friction coefficient, distance between cylinders have been investigated.

Key Words *:oscillation, frequency, rotating cylinders, simulation*

1 Introduction

This experiment is about the motion of a massive object placed into two identical parallel horizontal cylinders which rotate with the same angular velocity, but in opposite directions. When the cylinders start to rotate, the massive object will oscillate horizontally. Kinetic friction, friction coefficient and frequency of the rod have been investigated (Robin Hena and Et al.) also energy based solution and the turning and stopping points have been presented by Avi Marchewkaa and Et al. but they emphasized on the amplitude of the oscillator damping by a constant magnitude. In this study other different parameters are investigated too.

2 Experimental Setup

An aluminum rod is used as a massive object and two-car pulleys (with 8cm diameter) placed on two rods . A Van de Graaff generator belt is used to connect the cylinders. The belt was applied crossed over the cylinders to provide the opposite direction movement. Van de Graaff generator belt has low elasticity and friction doesn't make it warm so it can decrease errors. Three holes are used to change the place of the second cylinder as parameter. A sewing motor is used to change the speed of the cylinder. I've used speed controlling device to control the speed. Whenever It was pulled, speed is increased (Figs. 1 and 2).

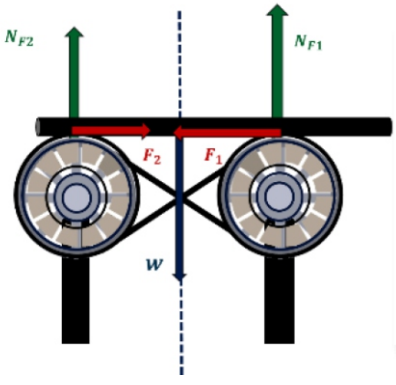

Fig. 1: Friction Oscillator Moddeling

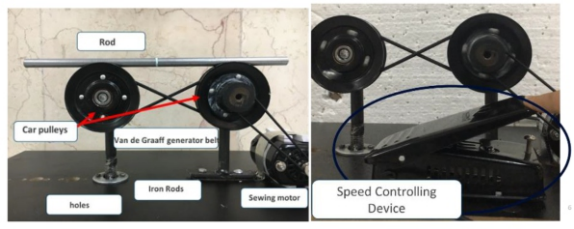

Fig.2: Experimental Setup

3 Theory

3-1 Amplitude of the Oscillation

There are three forces affecting the rod ; Normal force, friction, and weight. When the rod starts to move the weight applied on one of the cylinders will be more than the other one so it makes one of the normal forces to be greater. As a result, the friction in one point will be greater than the friction in other part so the rod will move toward opposite direction and this frequent occurrence makes the oscillation.

When the rod is placed exactly in the middle, it makes the frictions to be equal to each other so the rod will remain standing on its place. But in experimental result this will rarely happen so we can consider that the rod will always start to move. In order to investigate this phenomenon theoretically the friction must be calculated.

According to the Newton's second law the forces can be written (Eq. 1).

$$mg = N_1 + N_2 \quad (1)$$

and according to the torque , the normal force in each side is given by equations (2-4):

$$N_1\left(\frac{d}{2} - x\right) = N_2\left(\frac{d}{2} + x\right) \quad (2)$$

then:

$$N_1 = mg\frac{d + 2x}{2d} \quad (3)$$

$$N_2 = mg\frac{d - 2x}{2d} \quad (4)$$

By these normal forces, frictions can be calculated as well

(Eq. 5).

$$F = -\mu_1 N_1 + N_2\mu_2 = \frac{mg}{2d}(-\mu_1 d - \mu_1 2x + \mu_2 d - \mu_2 2x) \quad (5)$$

The place of the rod can be calculated by equation (6) which X_0 is the place that summation of the forces affecting the rod is zero. It is the place that frictions are equal to each other. X_0 Will be in the middle of the cylinders where the friction coefficient of the cylinders are the same. δ is distance of the rod from X_0 . Second derivation of X_0 is equal to the second derivation of δ because X_0 is constant (Eq. 7).

$$x = x_0 + \delta \quad (6)$$

$$\ddot{x} = \ddot{x_0} + \ddot{\delta} = \ddot{\delta} \quad (7)$$

Then:

$$F = m\ddot{x} = m\ddot{\delta} \quad (8)$$

$$\ddot{\delta} = \frac{g}{2d}((\mu_2 - \mu_1)d - (\mu_1 + \mu_2)2x_0 - 2\delta(\mu_1 + \mu_2)) \quad (9)$$

$$x_0 = \frac{d}{2}\frac{\mu_2 - \mu_1}{\mu_1 + \mu_2} \quad (10)$$

$$\ddot{\delta} = -\frac{g}{d}\delta(\mu_1 + \mu_2) \quad (11)$$

By solving the differential equation the place of the rod can be achieved in each second (Eqs. 12-15).

$$\delta = A\cos\omega t + B\sin\omega t \quad (12)$$

$$x = x_0 + A\cos\omega t + B\sin\omega t \quad (13)$$

$$A = x - x_0 \qquad B = \frac{V_0}{\omega} \quad (14)$$

$$x = x_0 + \left((x - x_0)^2 + \frac{V_{(0)}^2}{4\pi^2 f^2} \right)^{\frac{1}{2}} \cos(\omega t + \varphi_0) \quad (15)$$

In our experiments friction coefficient of the cylinders are the same. *Xo* have been considered 0 in both experimental and theoretical results. No velocity have been given to the rod in first situation in order to omit the V_0. By omitting V_0 φ_0 will be crossed out as well. So it shows that wherever the rod is placed in the first situation X_0 will be the amplitude of the oscillation.

3-2 Frequency of the Oscillation

ω and frequency are calculated as equations (16 and 17) :

$$\omega = \sqrt{\frac{g(\mu_1+\mu_2)}{d}} \quad (16)$$

$$f = \frac{\sqrt{\frac{2g\mu}{d}}}{2\pi} = \frac{1}{\pi}\sqrt{\frac{g\mu}{2d}} \quad (17)$$

According to the frequency formula, only friction coefficient and distance between two cylinders can affect this phenomenon. As much as distance between cylinders increases the frequency will decrease and as much as friction coefficient increases the frequency increases too.

4 Experimental Procedures

Different parameters are investigated in this experiment. Length of the rod, angular velocity of the cylinder and mass of the rod have no important role and don't affect the frequency as it is shown in Figures (3-5).

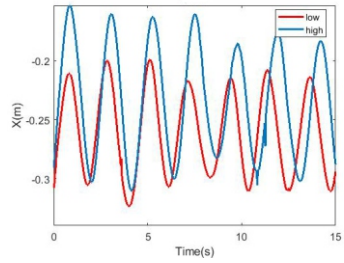

Fig. 3: Place of the rod versus Time in two different angular Velocities of the cylinders (low and high)

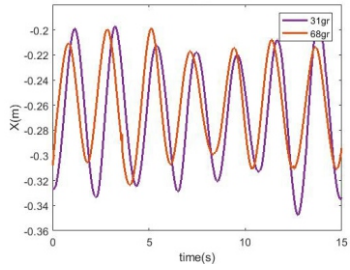

Fig. 4: Place of the rod versus Time in two different masses of the rod (31 and 68 gr)

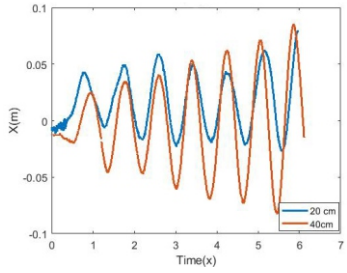

Fig. 5: Place of the rod versus Time in two different lengths of the rod (20 and 25 cm)

According to the equation (17) three affective parameters have been considered. These parameters are distance between two cylinders, friction coefficient between the rod and the cylinder, and the slope between the set up and the ground .

It is shown as much as friction coefficient between the rod and the cylinder increases the frequency will increase too (Fig. 6).

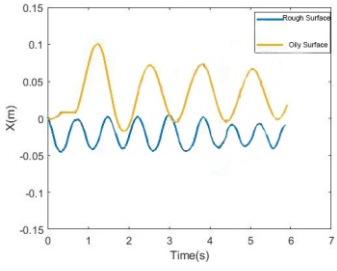

Fig. 6: Place of the rod versus Time in two different surfaces (oily and rough)

According to experimental data and equation (17), as much as distance between cylinders increases frequency will decrease (Fig. 7).

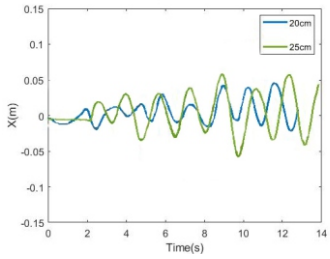

Fig. 7: Place of the rod versus Time in two different distances between cylinders

5 Simulation

The theoretical and experimental results of this phenomenon have been simulated by Matlab. The amplitude of the oscillation is an input in the simulation and the frequency is calculated from equation (17).

The outputs of the simulation gives the place of the rod in each second and a chart that compare the frequency and amplitude in experimental and theoretical results (Fig. 8).

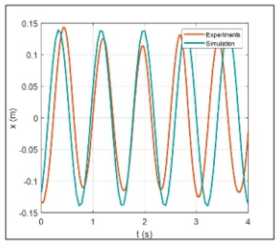

Fig. 8: Place of the rod versus Time , Comparison between simulation and experiment

It has been considered that the amplitude is constant and equal to the initial distance from X_0 but duo to the errors it is not always constant and might change . In ideal system the Normal forces must just affect the rod from the below but in experimental setup the Normal force on the rod is applied on the corners as well and that can cause some errors (Fig. 9).

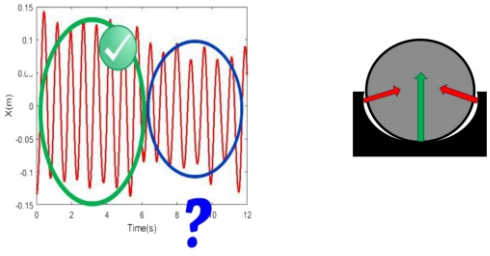

Fig. 9: Fluctuations in amplitude due to the errors in experiments

To decrease these errors, motor was used so the speed of the cylinders increased a lot and both the rod and cylinders didn't move with each other. That caused a usability in the movement of the rod which change the amplitude of the oscillation.

6 Conclusion

By investigating the forces which are applied on the rod, a differential equation has been achieved which shows frequency and amplitude of the oscillation.

According to experimental data and equation (17), frequency will decrease by increasing the distance between cylinders and increases by increasing the friction coefficient between the rod and the cylinder (Figs. 10 and 11).

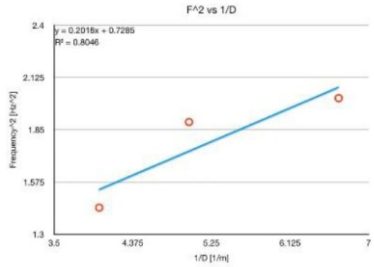

Fig 10. Frequency by changing the distance between two cylinders (Theory vs Experiment)

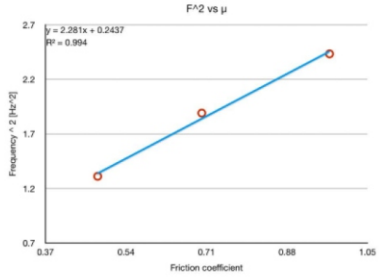

Fig 11. Frequency by changing the friction coefficient (Theory vs Experiment)

References

[1] D. Russell (2013), "The Friction Oscillator "[Video].

[2] R. Henaff et al , (2017), "A study on kinetic friction"

[3] E. Zeleny (2013), "The Friction Oscillator"

[4] R. Henaff, G. Le Doudic, and B. Pilette (2018), A study of kinetic friction: The Timoshenko oscillator American Journal of Physics 86, 174

Investigating a Falling Tower by Building a Robot

Arsalan Firoozkoohi *, Mahan Fallahpour, Alghadir high school, Kish Island/ Iran

ARTICLE INFO

Participated in Online MCTEA 2020, Brasil

Accepted in country selection by Ariaian Young Innovative Minds Institute , AYIMI

http://www.ayimi.org ,info@ayimi.org

ABSTRACT

Identical discs are stacked one on top of another to form a freestanding tower. The bottom disc can be removed by applying a sudden horizontal force such that the rest of the tower will drop down onto the surface and the tower remains standing. This phenomenon has been investigated and the conditions and the most important parameters which allow the tower to remain standing are found. By using free body diagram the identical forces are explained and in MATLAB more comparative and accurate measurements related to various angular accelerations are measured.

Key Words :*discs, forces, measurements, angular acceleration*

1 Introduction

Towers as tall structures are specifically distinguished from buildings in that they are built not to be habitable but to serve other functions using the height of the tower.In this research we are going to study the movement and balance of a tower which is built by different discs stacked on top of each other .

2 Theory and Methods

In this experiment there are different conditions as follows:

a) When the force is applied quickly to the bottom disc, without friction most probably you can see the rest of the tower will drop down on to the surface and the tower remains standing (Fig. 1).

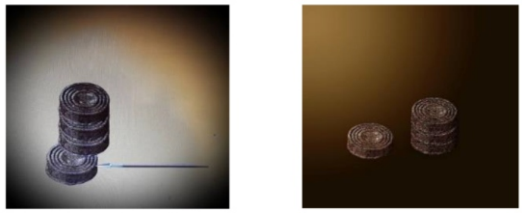

Fig. 1: Standing tower when the force is applied quickly to the bottom disc

b) When the force is applied slowly to the bottom disc most probably the rest of the tower will drop down on to the surface and the tower does not remain standing (Fig. 2).

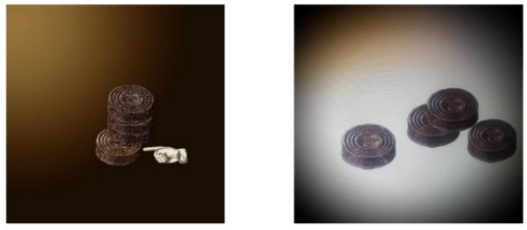

Fig. 2: Disturbing the balance of the tower when the force is applied slowly to the bottom disc (without friction)

c) When the force is applied quickly, with friction the rest of the tower will drop down on to the surface and the tower remains standing but with displacement in the discs (Fig. 3).

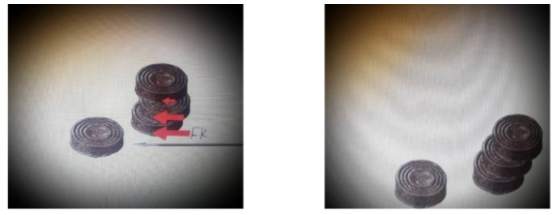

Fig. 3: Displacement in the discs by considering the friction

2 Basic Theory

All the applied forces are shown by using free body diagram (Fig. 4).

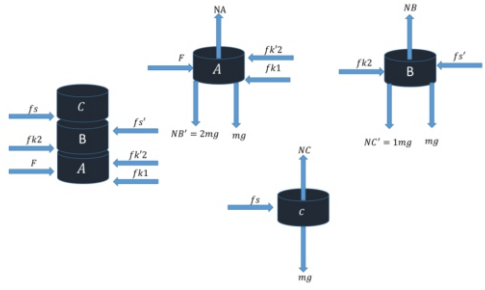

Fig. 4: Free body diagram and forces on the discs

First, we exert the force F to disc A, without gravity, the ower box moves in the same direction of the force and the ıpper disc stands unmoving. The friction force between the :arth and disc A is f_k . But with gravity force, the upper box vill accompany the lower box to some distance. It means hat the force will push this box forward in the same lirection of the exerted force. This force is called f_{k2} and is exerted on disc B. Similarly, the opposite force on disc A is called f_{k2} . These forces are the same for the disc above disc B (disc C) and all are calculated as follows (Eqs. 1-3) .

$$\sum fx = F - fk1 - fk2' = F - (\mu k.3mg + \mu k.2mg) \quad (1)$$

$$= F - 5\mu k.mg = ma\,, a = \frac{F}{m} - 5\mu k.g$$

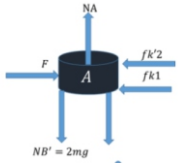

$$\sum fx = fk2 - fs' = \mu k.2mg - ma \qquad (2)$$

$$= ma\,, \mu k.2mg = 2ma\,, a = \mu k.g \qquad fs = fs' = ma$$

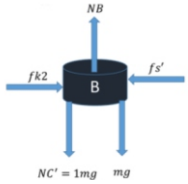

$$\sum fx = fs = ma\,, fs \le (\mu s) \times NC\,, \sum fx = ma \le (\mu s) \times mg\,, a \le (\mu s)g \qquad (3)$$

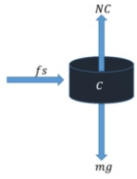

Rotational speed $\varpi = \frac{\Delta\theta}{\Delta t}$ and angular acceleration α in this phenomenon are the main parameters should be calculated and measured accurately (Eqs. 4-7).

$$D = z = x - \frac{\omega}{2}\,, \tau = f.D = mg \times \left(x - \frac{\omega}{2}\right) = mgx - mg\frac{\omega}{2} \qquad (4)$$

$$I = Icom + md^2 = \frac{1}{12}m\,(\omega^2 + h^2) + m\,((x - \frac{\omega}{2})^2 + (\frac{h}{2})^2\,) \qquad (5)$$

$$\sum M = I\alpha,\ \tau = I\alpha\ \,, mgx - mg\frac{\omega}{2} = \qquad (6)$$

$$(\frac{1}{12}m\,(\omega^2 + h^2) + m\,((x - \frac{\omega}{2})^2 + (\frac{h}{2})^2) \times \alpha$$

$$\alpha = \frac{mgx - mg\frac{\omega}{2}}{\frac{1}{12}m(\omega^2 + h^2) + m((x - \frac{\omega}{2})^2 + (\frac{h}{2})^2)} \qquad (7)$$

By MATLAB program more comparative and accurate measurements are done. By coding various angular accelerations and changing the displacement (x), different accelerations are measured. As demonstrated here, a linear diagram was obtained from this relation (Fig. 5).

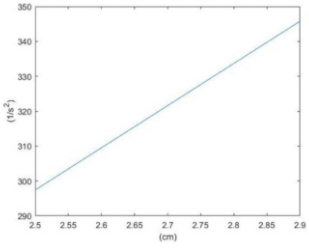

Fig. 5: Angular acceleration versus displacement

3 Experimental Setup

To reduce errors a robot was built (Fig. 6).

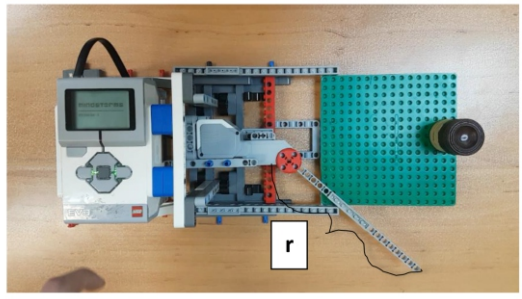

Fig. 6: Experimental setup

Angular velocity (ω) and v are calculated according to $\varpi = \frac{\Delta\theta}{\Delta t}$ and $v = r\omega$ then the probability of falling the discs is investigated (Fig. 7).

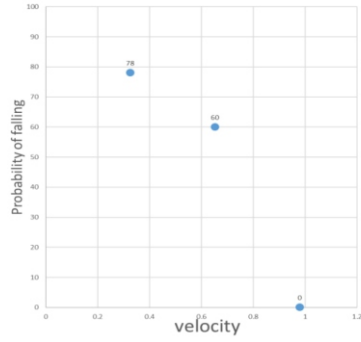

Fig. 7: Probability of falling versus velocity

It is clear by decreasing the velocity, the probability of falling increases. On the other hand, as the number of the discs increases, the probability of falling increases too (Fig. 8).

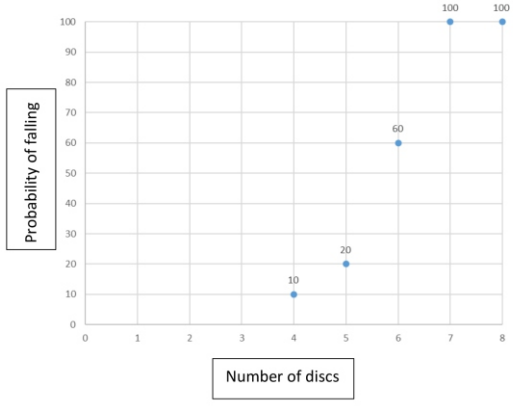

Fig. 8: Probability of falling versus the number of discs

By increasing the height of the discs in different experiments the possibility of falling was zero on the first two experiments. When the height of the discs are tripled, the possibility of falling was increased up to 50%. Finally, When the height of the disc was quadruplicated the possibility of falling raised to 100% (Fig. 9).

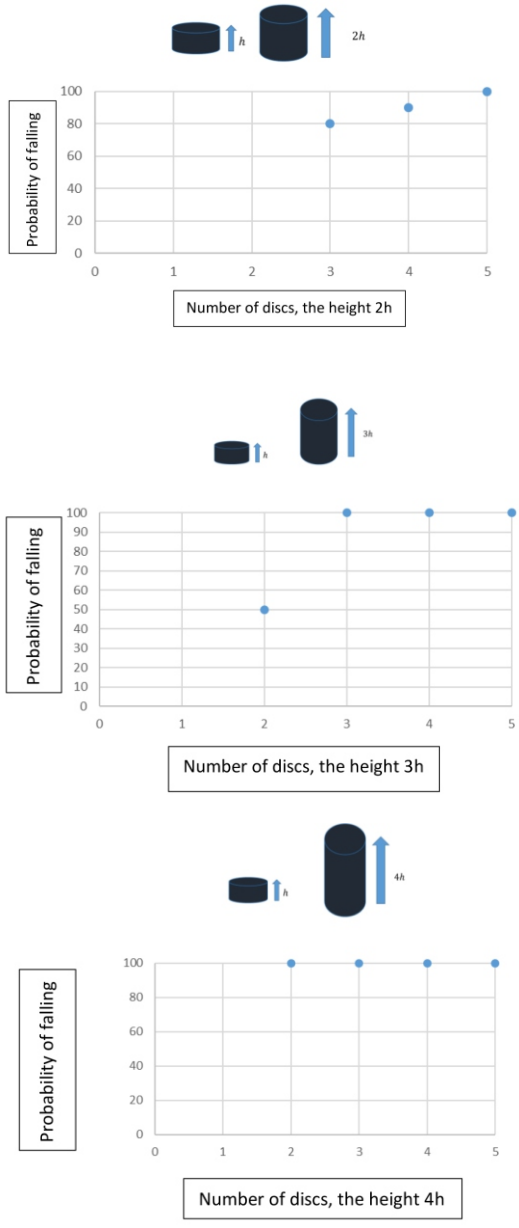

Fig. 9: Probability of falling versus the number of discs in different heights

4 Results and Conclusion

As shown, by increasing the height of the discs in various experiments, the possibility of falling is more. It is also needed to point out that the diameter of all discs is 3cm. Accordingly, when the height of the discs increased over 3cm, the possibility of falling raised to 100%. By increasing the height, the angular acceleration also increases. In conclusion the probability of falling is more when the altitude is higher so the angular acceleration is faster.

References

[1] D.Halliday , R.Resnick ,J.Walker (1923). Fundamentals of Physics. John Wiley & Sons.

Building and Studying an Electrostatic Motor

Mahsa Geramimanesh, Farzanegan 2 High School, Tehran/Iran, geramimanesh@gmail.com

ARTICLE INFO

Participated in IYPT 2019, Poland and Winner of Bronze Medal

Accepted in country selection by Ariaian Young Innovative Minds Institute , AYIMI

http://www.ayimi.org ,info@ayimi.org

ABSTRACT

For building a simple electrostatic motor which its propulsion is based on corona discharge, we used a rotor with 4 electrodes with sharp blades on them. By attaching them to the Van de Graaff and a power supply, the rotor could rotate in its place. To optimize the setup, the effect of different parameters such as the angle of the electrodes, diameter of the rotor, number of the electrodes or the distance between the electrodes have been investigated and the rotor reaches the maximum speed at a fixed input voltage.

Keywords: *electrostatic motor, Corona discharge, electrodes, rotor*

1 Introduction

Despite the multitude of patents on electrostatic engines, researchers recognize that data on the rotation of an engine rotor and its interaction with a "stator" are not yet sufficient for rapid development in this area [1].

We have two types of motors, first the electromagnetic ones, which the rotation of the rotor is based on motor's magnetic field and electric current which nowadays they use this types of motors in industry much more than the other type which is the electrostatic motors. Rotation of the electrostatic motors, is just based on electric current.

The first electric motor invented was a corona-based electrostatic motor (ESM) and it was about 100 years before the conventional magnetic motor was conceived. The ESM is characterized by simplicity of construction without winding and lightweight. The influence of corona electrodes' configurations on output torque was experimentally investigated in ESM with multi-blade electrodes. The motor fabricated consisted of a 100 mm diameter hollow cylindrical rotor made of acrylic resin as a dielectric and several knife-blade corona electrodes with 100 mm length [2]. We built an electrostatic motor which with a fixed input voltage, it will reach the maximum angular velocity which is based on corona discharge and causes the air molecule to be ionized. The same charges of the electrode, will accumulate on the rotor and with the attraction of the opposite charge on the next electrode and the repulsion of the similar charge, the rotor will rotate.

2 Experimental Setup

Our experimental setup consists a Van de Graaff, power supply, four electrodes with sharp blades on them, and a rotor which itself is a plastic cylinder that has an aluminum shield inside it (Fig.1).

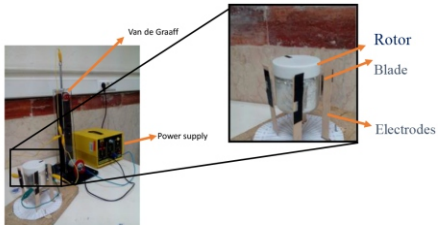

Fig 1: Corona Motor Experimental Setup

The electric field doesn't penetrate in the metal area so in the fixed voltage, larger angular velocity will be observed because it's like we are decreasing the distance between two electrodes. When the electrodes are attached to the opposite charges of the Van de Graaff and Van de Graaff to the power supply, the rotor will start to rotate. Two electrodes in front of each other will gain similar charges which means every electrode next to each other have opposite charges with each other. These blades with opposite charges on them and the electric field around the charges, due to the corona discharge, will cause the air molecules to ionized and the both charges in one molecule will be separated [3].

Full paper has been published in:

Lat. Am. J. Phys. Educ. Vol. 14, No. 2, June 2020

http://www.lajpe.org

(1)

Analysis of Factors Affecting the Taste of a Food

Artin Radmatin , Vale School, Tehran/Iran

ARTICLE INFO

Participated in IMSEF 2020 and Winner of Gold Medal in junior section (11 years old), Turkey

Accepted in country selection by Ariaian Young Innovative Minds Institute , AYIMI

http://www.ayimi.org ,info@ayimi.org

ABSTRACT

Saliva in our mouth helps to identify different tastes. It is very important to separate the nature of the sense and perception of the taste. Sense is the act of receiving stimuli by organs. In this research, we first examined the structure of the sense of the taste and its perception mechanism in humans. Then, two quantitative parameters were selected: Food Temperature and the number of the chewing of the food in our mouth.The test was done with the statistical community based on the determined parameters. The statistical community were selected from 1 to 14 years, 15 to 24 years, 25 to 44 years, 45 to 64 years and 65 years and over.

Keywords: *mouth, saliva, sense of taste, statistical community*

1 Introduction

Mouth is the first organ of digestive system with tongue and saliva which make the sense of the taste . Saliva dissolves food in the mouth and activates specific taste receptors and the perception of tastes depends on the tongue .

Also about the sense of taste, we can say that the sense of taste is the stimulation of the taste buds by food stimuli. Some people think, perceiving and feeling the taste are the same but it is not correct .

Feeling the taste is act of receiving stimuli by the sensory organs, while perception is the act of recognizing and interpreting sensory information recorded in the brain.

After learning about the mechanism of sense of the taste, we are going to tell about the factors that can affect the taste of our foods. The first thing that is very important about the taste is that it is not just the sense of taste helps to identify the tastes and also the sense of vision and sense of smell help a lot to identify the tastes but we didn't focus on this topic because this topic was largely proven before.

Also some Human characteristic feeling that affect the taste of food are human taste and indoctrination. Human taste is acquired and it may change in different ages.

Indoctrination is a psychological pressure on human beings that can prepare the human mind to accept things that may be unreal; for example, when it is said the pepper is very spicy and consist on it, however if the pepper isn't spicy, after eating you may say it is spicy.

About the different flavors that human can identify we can say there are a lot of tastes but the seven flavors are known completely by scientists, as follows (Fig.1):

Fig.1: picture of where every taste is felt

1-Saltiness like salt
2- Sourness like sour lemon
3- Bitterness like dark chocolate
4-Astringent like persimmon
5- Sweetness like sugar
6- Spiciness like spicy pepper
7- Umami like tomato (Umami is Japanese and means " a pleasant savory taste")

2 Experiments

First Step: after talking with a nutritionist, an experiment was done to find out more about this problem.

Second Step: we made a diet soup with some tastes like sweetness which was from the carrot, and a very low taste of sourness and saltiness.

Third Step: then our groups were selected according to the statistical groups based on searching on website. Our statistical population was 40 people both in different ages and different genders.

Fourth step: the prepared soup was evaluated by the statistical population based on the determined parameters. The statistical population should give scores between 1 to 4 to their tasting power about each flavor and should write some sentences about tasting different flavors and their general feelings when they eat the soup.

2-1 Determined Parameters

Parameters which were considered in our experiments are as follows:

1- Temperature of the foods:
The prepared soup was tested once hot (80°C) and once cold (30°C)by the statistical population .

2- The count of chews:
The prepared soup was re-tested by the statistical population , once with a low number of chews (Lower than 10 chews) and the other with a high number of chews (More than 10 chews).

2-2 The Meaning of Each Scores

All scores are described as table (1) which is the feeling of the tastes in our statistical population from 1-4 (The prepared soup was used).

Table 1: Scores' Definition

1	Feel the taste less than itself
2	Feel the taste accurate
3	Feel the taste a little more than itself
4	Feel the taste more than itself

2-3 The Statistical Population

According to standard age groups, we selected our statistical population as Table (2).

Table 2: Statistical population

Age groups / Information	Age group of 1 to 14 years (Children)	Age group of 15 to 24 years (Youth)	Age group of 25 to 44 years (Adult)	Age group of 45 to 64 years (Middle-aged)	Age group of 65 years and over (Seniors)
Number of people in each group	10	5	13	7	5
Number of women in each group	3	2	9	2	3
Number of men in each group	7	3	4	5	2

3 Results

Group (a) age of 1 to 14 years old:

1-Taste recognition power is very high in this age group.
2-The number of chews was ineffective in detecting tastes.
3- The delicate flavors were less pleasant for this group.

Group (b) age of 15 to 24 years old:

1-The warming of the food helped to identify the taste and appetite of the food.
2- Delicate and mild (slightly spicy) flavors are relatively pleasant for this group.

Group (c)age of 25 to 44 years old:

1-Taste recognition in this age group was high in both genders when food was hot.
2-The number of chews was ineffective in detecting tastes.
3-The men felt the sour taste more and didn't like it, but the woman enjoyed it more when they could taste the sourness and saltiness of the food.

Group (d) age of 45 to 64 years old:

1-Taste recognition was very weak in women in this group and much more accurate in men.
2-The warming of the food helped to identify the taste and appetite of the food.
3-The number of chews was ineffective in detecting tastes.

Group (e) age of 65 and over:

1-The taste detection power of this group was very weak.
2-The number of chews was ineffective in detecting tastes.
3- The warming of the food helped us to identify the taste and appetite of the food.
4-There was no change in taste detection power between men and women.
These results are compared in different groups between Men and Women as shown in Figure (2).

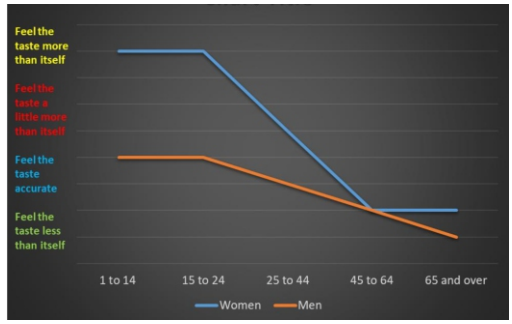

Fig. 2: Results'Diagram

The scores in each group are shown in table (3).

Table 3: Scores in Each Group

Age groups / Scores	1	2	3	4
1 to 14	0women 1 man	0 women 4 men	0women 0 men	3women 2 men
15 to 24	0 women 0 men	0 women 2 men	0 women 1 man	2women 0 men
25 to 44	0 women 3 men	0 women 1 man	6 women 0 men	3 women 0 men
45 to 64	2 women 4 men	0 women 1 man	0 women 0 men	0 women 0 men
65 and over	2 women 2 men	1 woman 0 men	0 women 0 men	0 women 0 men

4 Analysis Results

1- Being a family member had a great impact on recognizing tastes. Because in all age groups in one family, their views were almost the same.

Possible reason: Habit of a fixed family food taste (approximately 90%)

2-Effect of Indoctrination: according to the analysis , we can say that indoctrination has effect on tasting the food. (approximately 8%)

3-In obese people who wanted to lose weight and have a diet, losing weight thoughts had affected on tasting the food taste

5 Conclusion

1-Warming of the food had affected a lot on the tastes of food . When the food was warm, the food was more pleasant for the people.

2- The count of chews had no affect on tasting the food .

Acknowledgments

Thanks to Buca IMSEF organizers and both Mr. Arjmand in Vale school and Dr. Izadi in AYIMI.

References

[1] https://fa.parsiteb.com

[2] https://www.yjc.ir/fa/news/6957843

[3] http://farzanrad.com/index.php/what-is-taste

[4] https://www.oviro.com/mag/29169

[5] https://www.zoomit.ir/2012/10/10/3274/taste-sense-taste/

[6] https://fa.parsiteb.com

BUBBLES' OSCILLATIONS IN LIQUIDS

Bahar Aghazadeh , Farzanegan 5 high school, Tehran/ Iran, baharaghazadeh5@gmail.com

ARTICLE INFO

Participated in IYPT 2019 , Poland and winner of Bronze Medal

Accepted in country selection by Ariaian Young Innovative Minds Institute , AYIMI

http://www.ayimi.org ,info@ayimi.org

ABSTRACT

When a container of liquid (e.g. water) oscillates vertically, it is possible that bubbles in the liquid move downwards instead of rising. As the bubble moves downward, the pressure of the water increases and the volume of the bubble will decrease. Then the added mass decreases and the bubble accelerate downward. But when the bubble moves upward, the volume and the added mass will increase, and pressure decreases so the acceleration will decrease. The point is that every time when the bubble moves up; because of low acceleration, it will not go to its initial place. It means in each oscillation the bubble effectively goes down.

Keywords: *liquid , oscillation, bubbles, pressure*

1 Introduction

It was found in experiments in the late 1950s that, under certain circumstances, bubbles would remain suspended or even sink to the bottom of the tank. It has been suggested that this phenomenon could be a cause of early rocket failures due to collecting bubbles interfering with fuel sensors as they are cylindrical and vibrating vertically in the rockets and causing premature stage separation [1]. Bubble media are actively used in the processes of purification of melts by the passage of insoluble gas bubbles through them. Bubbles are believed to be insoluble in the liquid. The effects occurring at the interface between a bubble and the liquid and the kinetics of bubble merging are excluded from consideration [2].

2 Experimental Setup

To do our experiments we used a 4-ohm speaker as the vibrating device which the dust cap is removed, a 30-watt amplifier, containers with 2.5 cm in diameter and different heights (6, 7.4, 10.5, 12.1 cm) and caps. To place the containers on the speaker, they were stuck to a cap and put in the cavity of the speaker (Fig. 1).

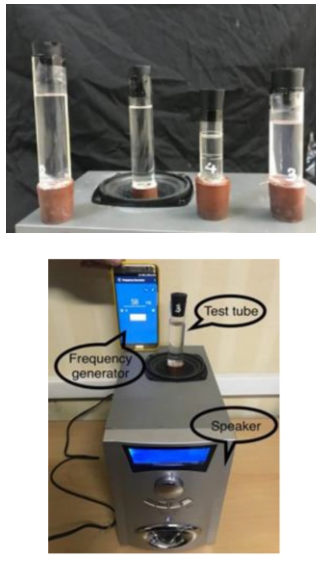

Fig. 1: Experimental Setup

3 Methods and Theory

We consider the container oscillates with amplitude "A" and "ω" which the position of the container is $x = A\sin\omega t$ and its acceleration is $\ddot{x}$. The total acceleration of the bubble is the sum of gravity and the acceleration of the vibration (Eq. 1-3). The data analysis will be by tracking the bubbles (Fig. 2).

$$\text{Displacement}=x = A\sin\omega t \quad (1)$$

$$\text{Sinusoid alacceleration}=\ddot{x} = A\omega^2\sin\omega t \quad (2)$$

$$\text{Total acceleration}=g + A\omega^2\sin\omega t \quad (3)$$

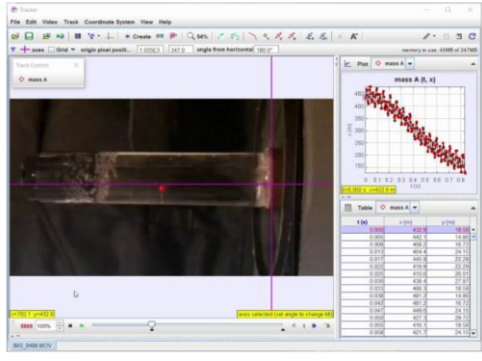

Fig. 2: Tracking the bubbles in our experimental setup

Full paper has been published in:

Lat. Am. J. Phys. Educ. Vol. 14, No. 2, June 2020

http://www.lajpe.org

PEPPER POT

Sahar semsarha , Farzanegan 2 high school, Tehran/ Iran, sahar.sems@gmail.com

ARTICLE INFO

Participated in O-IYPT 2020 , Georgia

Accepted in country selection by Ariaian Young Innovative Minds Institute , AYIMI

http://www.ayimi.org ,info@ayimi.org

ABSTRACT

In this essay, the motion of the particles inside a container have been investigated. When something is rubbed along the bottom of the container, the amount of the particles pouring out will increase. In this paper the main reason of the phenomenon has been explained and also some affective parameters such as the particle poured inside the contain, the area of the holes of the container have been investigated.

Key Words :*particles, container, motion, affective parameters*

1 Introduction

This experiment is about the motion of particles inside a pepper pot. If we shake a paper pot, number of the particles poured out will be low but if we rob something along the bottom of it this amount will increase. In this paper, a method had been presented to investigate in which cases the amount of pouring out the particles will be higher.

The main reason that this amount increases is because of vibration which is applied to it from rubbing. When we rub the pepper pot the agglomeration cannot happen between the particles so the amount of pouring out increases.

Some parameters can affect this vibration. These parameters contain the scrubs speed, the hoppers material and the geometry of the particles.

2 Experiments and Methods

A motor on a stand has been used to rob the pepper pot. The angular velocity of the motor was constant. the material of the hopper was glass with a cylindrical shape (Fig. 1).

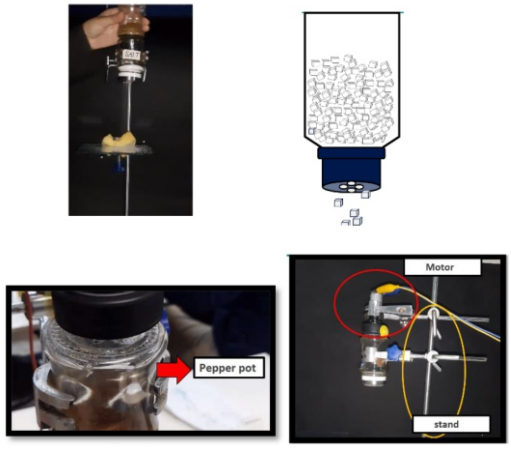

Fig. 1: Pepper Pot experimental setup

3 Theory

3-1 Agglomeration

In normal situation the middle atoms are dragged from all around but some energy is left on the surface atom which makes the Agglomeration, Van der Waals forces between the particles, to happen (Fig. 2).

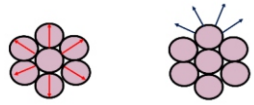

Fig2: Energy on the surface of the particle

That means the small particles will merge and make a bigger particle which cannot pass through the holes of the pepper pot easily (Fig. 3).

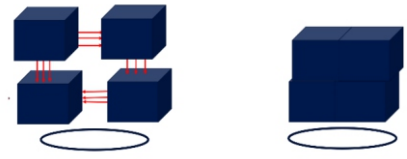

Fig 3 : Agglomeration making bigger particles

In normal situation, when we shake the pepper pot the agglomeration will cause the amount of pouring out to decrease. The motion of the particles had been investigated in vibrating system (Fig. 4).

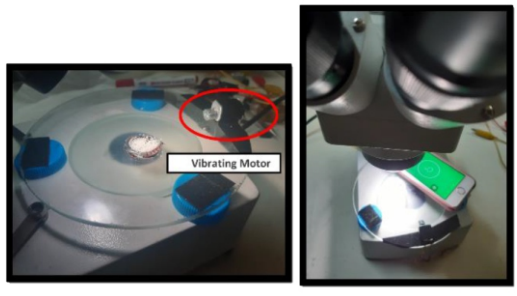

Fig 4 : Investigating the motion of the particles in vibrating systems

The particles want to be in the least energy possible. The least energy possible is in the most symmetrical state.

When the vibration is applied to them from the vibrating system, the particles are able to move and be in the most symmetrical state. So they will decrease the free space left on the surface and spread all around (Fig.5a and b). There will be some distance between the particles and the particles will move permanently. So in vibrating systems, the agglomeration cannot happen.

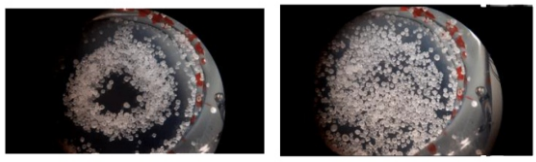

(a) (b)

Fig5: a) Particles before the vibration ; b) Particles after the vibration

It is approximately the same in the pepper pot. When the pepper pot is robbed, waves will be formed. This waves decrease the agglomeration so the particle will not merge and they will cover the hole. Therefore, the amount of pouring out increases (Fig. 6).

Fig. 6: Waves formation

3-2 Mass

Number of the particles over area had been defined as a variable (Eq. 1):

$$n = \frac{Number\ of\ particles}{Area} \qquad nA = N \qquad (1)$$

where A is the area of the holes. To solve this problem, the acceleration of layer pouring out must be considered constant. That means, the layers of the particles must affect each other so the mass of the particles poured inside the pepper pot (which affect the number of this layers) cannot affect this phenomenon. Therefore, mass poured out in each second will be constant. by adding the coefficient α to the equation the mass poured out in each second is found (Eq. 2).

$$\dot{N} = \propto nA \qquad (2)$$

The particles are covering all around the hole so they cannot affect each other and the only external force which is affecting the particle passing through the hole is gravity. Then (Eq. 3 and 4):

$$\dot{M} = \dot{N}m = \propto nAm = \beta \qquad (3)$$

$$M = M_0 - \beta t \qquad (4)$$

According to these equations the effective parameters are the particles we pour inside the pepper pot and the number of the holes which can affect the area.

4 Experimental Procedures

4-1 The Constant Acceleration

The constant acceleration of this layer have been investigated in experimental data to approve the consideration. As it had been mentioned in theory , by have a constant acceleration for each layer $\dot{M}$ will be constant. So the slope of the mass poured out per time must be constant and the trend line passing through experimental results, must pass through zero. Also the mass poured inside the pepper pot won't affect this phenomenon (if the acceleration of these layers are constant) . Then different mass poured inside the pepper pot have been investigated as one of the parameters.

According to Figure (7), changing the mass inside the pepper pot which affect the number of the layers, cannot affect this phenomenon and this approves that the acceleration of the layers is constant and the same till the end of the pouring out.

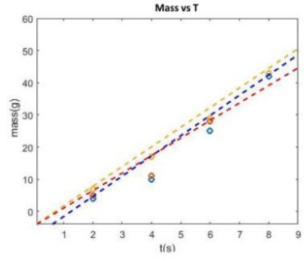

Fig 7: Mass poured out in each second versus time (different mass poured inside the pepper pot)

3-2 Affective Parameters

According to the equation (3) changing the number of the holes can affect the area and as much as number of the holes increases the mass poured out in each second will increase (Fig. 8).

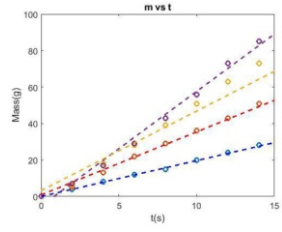

Fig 8: Mass poured out in each second versus time (area)

Three different particles have been investigated too. (salt, sugar, flixweed seed).

Particle	mass	dhole	Geometry	S
flixweed seed	1.88gr	1.53mm		$0.038163mm^2$
salt	6.6gr	1.53mm		$625mm^2$
sugar	0.37gr	1.53mm		$0.571536mm^2$

Fig 9: Experimental Results

Mass column gives us the mass poured out in each second. For example, in two seconds 1.88g seed and 6.6g salt came out from the pepper pot. This column gives us the ability to compare this particle experimentally. To compare the particles theoretically (Eqs. 5 and 6):

$$\varepsilon = \frac{S(empty\ space)}{S(total)} \quad (5)$$

$$A = \frac{N.S(particle)}{S(total)} = 1 - \varepsilon \quad (6)$$

When the amount of empty spaces decreases the number of the particles filling the hole will increase. But when we have large particles Ɛ will increase . So the number of the particles and mass poured out in the same time will decrease. For different particles:

$$A_{salt} = \frac{N_{salt} \cdot S_{salt}}{S_{total}} = N_{salt} \cdot R_{salt}$$

$$S_{total} = S_{hole} = \pi r_1^2$$

$A_{salt} = 24 \times 0.041 = 0.984$
$\mathcal{E}_{salt} = 1 - 0.984 = 0.016$

Fig 10: Salt particles inside the hole

and the same for other particles:

Fig 11: Flixweed seed particles inside the hole with Ɛ=0.187

Fig 12: sugar particles inside the hole with Ɛ=0.124

The shape of the particles will cause some mismatches in experimental and theoretical results. sugar is cubic and it has sharp apexes but seed doesn't have any apexes so it can pass through the hole easier. The name of this effect (effect of the shape of the particles) is steric effect. The steric effect must be considered in our results.

Some other particles had been investigated as well. Because pepper has sharp apexes it cannot pass through the hole easily and the amount of pouring out decreases.

But when it is filled with flour the amount of pouring out increases but not as much as it was expected because the $\mathcal{E}$ of the flour is low.

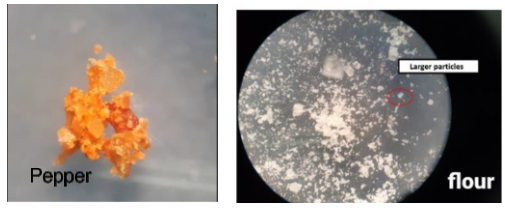

Fig. 13: Pepper and Flour particles

In equation (4) β is constant so the trend line passing through experimental results must pass through zero and theory versus experiment results are approximately matched.

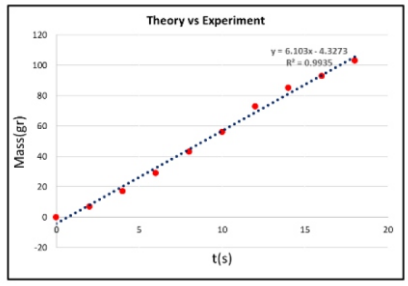

Fig. 14: Mass poured out in each second versus time (theory vs experiments)

4 Conclusion

Agglomeration was the main reason which made the amount of pouring out to be low in normal situation. All the experiments show agglomeration cannot happen in vibrating systems. The acceleration of the layers of different particles have been considered constant. The particles poured inside the pepper pot and the number of the holes are important parameters.

The shape of the particles as the steric effect was investigated too.

In theory the same as in experimental results it is found that the particles will cover all around the hole but in the end of the pouring out (in experiments) particles are not enough to cover all around the hole so the amount of pouring out decreases as an experimental error.

References

[1] D.Halliday , R.Resnick ,J.Walker (1923). Fundamentals of Physics. John Wiley & Sons.

[2] A. Wesley. , R. Feynman (1970). The Feynman Lectures on Physics Vol I.

[3] pp. Lavoisier, A.L. & Laplace, P.S. (1780)."Memoir on Heat", Académie Royale des Sciences

[4] Hadden, Richard W. (1994).On the shoulders of merchants: exchange and the mathematical conception of nature in early modern Europe.

[5] M. Weiss and J. Baez (2017). "Is Energy Conserved in General Relativity?". Retrieved 5 Jan

A Dual Efficiency Optical Instrument (Both Microscope & Telescope)

Shiva Mahdavisereshtl, Tehran/ Iran

ARTICLE INFO

Participated and was awarded in First Step to Nobel Prize as high school student (2006-2007)
postgraduate in Medical Science (present)
Accepted in country selection by Ariaian Young Innovative Minds Institute , AYIMI
http://www.ayimi.org ,info@ayimi.org

ABSTRACT

Both telescope and microscope are basically constructed using 2 planoconvex lenses. However, it is considerable that in telescopes the eye piece lens focal distance is shorter than the objective one while on contrary in microscopes the focal distance in eye piece lens is longer than the other. According to this fact, it seems that these 2 devices, telescope and microscope, are operating inversely.

Keywords: *telescope, microscope, lense, focal point*

1 Introduction

By development of science, research and investigations allocated a special place to itself. This is while measurement and dimensions play an important role in science and study. As we know for investigating huge and small objects, telescope and microscope are used respectively. An instrument composed of these 2 devices will definitely make working easier for researchers.

According to the fact that by placing 2 planoconvex lenses in front of each other and adjusting the distance between them, we can construct simple microscopes or telescopes. Certainly, by composing these 2 devices in telescope and microscope, it is possible to provide a two sided instrument performs both telescopic and microscopic operations.

2 Materials and Methods

2-1 Astronomical Telescope

Astronomical telescope is made of 2 planoconvex lenses. The objective lens makes a real inverted image of the object placed in infinity, in focal distance. Astronomical telescope is usually regulated in a way that the final image gets formed in infinity. For this result, the focal distance in eye piece lens (fe) should coincide with the focal distance in objective lens (fo) . In this instrument (fo) is long and (fe) is short. The final image is virtual , inverted with regard to the object and direct in comparison with the first image (Fig.1).

The following equation yields the angle magnification of telescope (Eq.1).

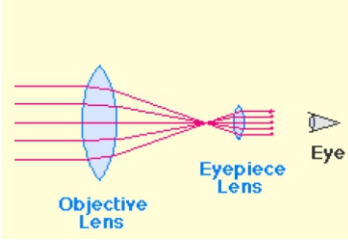

Fig. 1: Telescope

$$m = \frac{\beta}{\alpha} \qquad (1)$$

According to these description a telescope can be constructed as follows.

1. Planoconvex f=8.3cm
2. Planoconvex f=25cm as the objective lens
3. Ruler
4. Leg (pedestal)

The procedure for building this telescope is:

1. Put the ruler in a far distance.
2. Place the lens on the pedestals.
3. Use the lens with focal distance of 25cm as the objective one.
4. Place the lens with focal distance of 10cm in a distance of fe +fo=35cm .
5. While looking through the eye piece lens , adjust the distance between the objective and eye piece lens till the image become clear.
6. For better observing, we can use a light projector on the object.

Note that the final image is figurative and inverted with the object and get formed in infinity.

2-2 Microscope

This instrument is made of 2 lenses, one near to the object and the other near to our eyes. The focal distance of objective lens is indicated by fo and the object is placed between fo and 2fo. The image obtained is inverted, real and larger and get formed in the focal distance of eye piece lens . This image is as an object for the eye piece lens. So the final image is direct, figurative and larger with regard to the first image (Fig.2).

According to the description ,a microscope can be constructed.

Requirements:

1. A detracting transformer.
2. Light projector
3. Planoconvex lens f=8.3cm
4. Planoconvex lens f=25cm
5. Pedestal

The procedure for building this microscope is:

1. Connect the light projector to the transformer.
2. Draw small checkered lines on a paper and put it in front of the projector.
3. Put the objective lens in a distance of 4 cm to the paper.

4. Put the eye piece lens in a distance less than 55 cm to the first lens.

5. Look through the eye piece lens at the checkered paper and adjust the distance between lenses to obtain a clearer image.

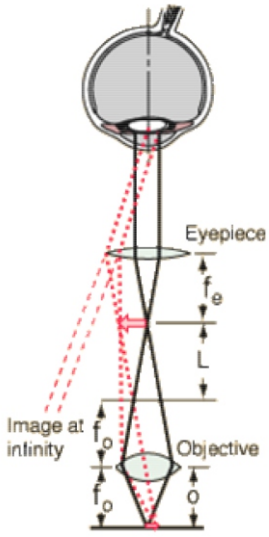

Fig. 2: Microscope

3 A Dual Efficiency Optical Instrument

As mentioned in previous sections both telescope and microscope are basically constructed using 2planoconvex lenses. However, it is considerable that in telescopes the focal distance of eye piece lens is shorter than the objective one while on contrary in microscopes the focal distance in eye piece lens is longer than the other. According to this fact, it seems that these 2 devices i.e. telescope and microscope is operating inversely. It means that by placing 2 planoconvex lenses in front of each other, in case we look through one side, this arrangement will have microscopic characteristics and if we look through the other side it will have telescopic characteristics. Of course it should be considered that distances between these 2 lenses , in 2 cases above, are not identical i.e. in telescopic case , lenses should be placed in a distance of fo+fe to each other while in microscopic case , the distance between lenses must be to some extent more. Thus, if we accumulate 2 planoconvex lenses in one device in a way that the distance between these 2 lenses become adjustable, then we will be able to obtain both telescopic and microscopic efficiency (of course basically) from device produced and through its 2 sides . So we proceed to construct a device (Fig3).

Fig 3: a dual optical instrument

The constructed device can perform in both telescopic and microscopic way (Figs. 4 and 5).

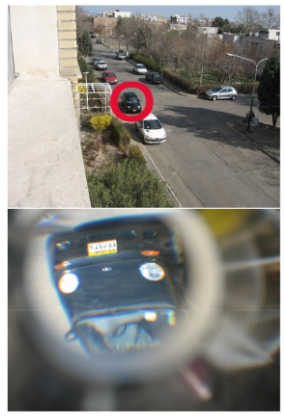

Fig 4: Image obtained from telescopic part

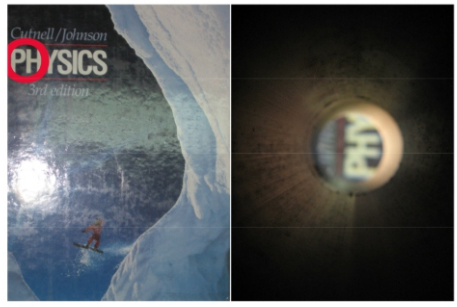

Fig. 5: Image obtained from microscopic part

4 Complementary Steps

Now, we should inspect if it is possible to use exhibited layout in progressive instruments. For this purpose, we should inspect that in basic level, how we can improve the magnification of a telescope or a microscope.

The magnification of a telescope and microscope are obtained from the equations (2 and 3) , respectively.

$$M(telescope) = \frac{-f_o}{f_e} \quad (2)$$

$$M(microscope) \approx \frac{-(L - f_e)N}{f_o f_e} \quad (3)$$

where N is human eyesight (naturally equal to 25cm) and L is the distance between 2 lenses which is always more than fo+fe.

So if L= fo+fe , then:

$$M(microscope) = \frac{cte}{f_e} \quad (4)$$

Considering equations(2) and (4), since in our device, the eye piece lens in telescope and the objective lens in microscope are the same and vice versa, in order to improve the magnification of the telescopic part of the device we should use an objective lens with a larger focal distance, while it results in decreasing the magnification of the microscopic part , considering :

$$f_e(miroscope) \equiv f_o(telesope)$$

So there would be an optimum point for our device construction , otherwise it will result in decreasing the magnification of one of these 2 parts.

5 Conclusion

1 – Using the exhibited layout and in an optimum point it is simply possible to construct a device which basically performs both telescopic and microscopic operations in a good way.

2 – In order to improve the magnification of both parts of the device (telescopic and microscopic) and to construct more progressive device , this fact should be considered that the magnification of these 2 parts are inversely related to each other . The only way to complete this device for more progressive operations is to combine microscopic and telescopic parts meanwhile the progressive equipment related to each one get applied separately in the device in a way that in each form of operation the equipment required enter into the circuit.

References

[1] Cutnell, J. D. and K. W. Johnson, (1995). Physics (3rd Edition, John Wiley & Sons, Inc.), 831-855

[2] Holliday, D. & R. Resnik, (1978). Physics, John Wiley &Sons, Inc.

Combination of Air and Water Pressure in Applied Fields

Mahsa Tajdari, Tehran/ Iran

ARTICLE INFO

Participated and was awarded in national competition (2007) student

PhD Candidate in Mechanical Engineering , Texas(present)

Accepted in country selection by Ariaian Young Innovative Minds Institute , AYIMI

http://www.ayimi.org ,info@ayimi.org

ABSTRACT

Our discussion of fluids has two parts, statics and dynamics. Fluid statics concentrates on the properties of fluids at rest, while fluid dynamics focuses on fluids in motion. There are static fluids in the hydraulic systems that transmit the large pressures. In this paper a hydrostatic system is recommended. This system is able to save the potential energy of water in a new procedure by using the combination of air pressure and pressure of the fluids. The potential energy of water in the back of the dams is utilized to produce electricity. So, using this recommended hydrostatic system, we can reuse the water exiting out of turbines in power plants.

Keywords: *air, fluids, pressure, potential energy*

1 Introduction

As we know, the atmosphere around the earth applies a pressure on the bodies. This pressure is called "Air Pressure" and is caused by the weight of the air which is located above the bodies. So far many different experiments have been performed about the air pressure. Perier (et.al) was the first one who accomplished many experiments and found out the effect of air pressure. Torichelli continued the Perier's studies and showed that the air pressure applies on all of the bodies. Pascal studied the Torichelli's works and he concluded that the amount of air pressure in the top of a mountain is less than the value of air pressure in the valley.

On the other hand, we know that all of the liquids apply a pressure on the bodies which are submerged in liquids. Many scientists like as Archimedes, Pascal and Bernoulli have performed many experiments about the pressure of liquids. Anyone who has tried to push a beach ball under the water has felt how the water pushes back with a strong upward force.

This upward force is called the buoyant force, and all fluids apply such a force to objects that are immersed in them. The buoyant force exists because fluid pressure is larger at greater depths. The hydrostatic properties of a liquid are not constant and the main factors influencing it are the density of the liquid and the local gravity. Both of these quantities need to be known in order to determine the hydrostatic pressure of a particular liquid [1,2,3].

In this paper, performing a series of experiments, is shown that we can save the pressure of liquids in the form of potential energy in a hydrostatic system. This energy with combination of air pressure can be used in many applied fields.

2 Experiments

2-1 Equipments of Experiments

According to (Fig. 1), a vessel is chosen including two throats. One throat (A) is wide and the other one (B) is narrow so that the section related to (B) throat is crisscross. Then (B) throat is closed with a cork completely.

2-2 Explanation of Experiments

In this case some water is poured into the (A) throat as shown in (Fig. 2).

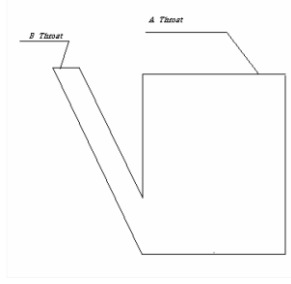

Fig. 1: Schematic of equipment used in the experiment

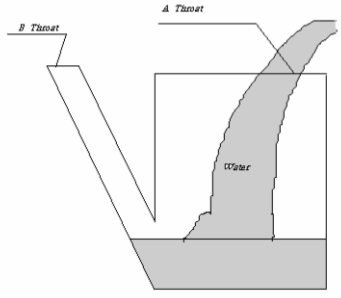

Fig. 2: Pouring some water into the vessel

Water rises in the vessel to the height of "h". If we continue pouring the water, the height of water in tube (B) remains constant while water rises in section (A) to the height of "H" as shown in (Fig. 3).

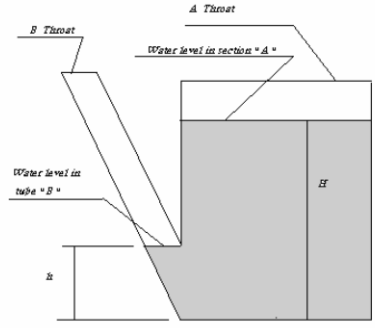

Fig. 3: The height of water in two sections of vessel

As shown in (Fig. 3), if we pick up the cork from the (B) throat suddenly, water barrels in tube (B). So, water slats out of the tube (B) as shown in (Fig. 4). As it can be seen, the height of (H) in section (A) will be reduced.

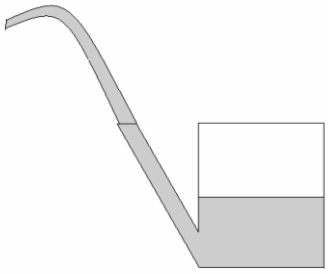

Fig. 4 :Water slats out of the tube (B) by removing the cork

3 Analysis of Experiments

As it can be seen in (Fig. 2), water rises in the vessel to the height of (h). Continuing the pouring of water, the height of water in tube (B) doesn't change while the height of water increases in section (A), because (B) throat had been closed with a cork completely and the air can not exit out of this tube. On the other hand, (A) throat had not been closed, so the air in this section can exit and water can be replaced. Therefore, the height of water increases as shown in (Fig. 5).

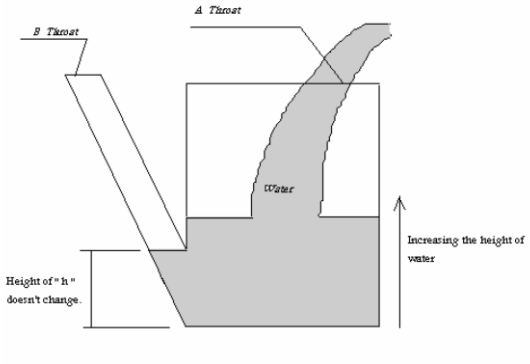

Fig. 5: Air is locked in tube (B)

Refer to (Fig. 6) and consider the points "C" and "D" on the water levels in (A) and (B) sections, respectively. The pressure of "C" and "D" points are equal because these points are located in a horizontal line. Thus we can write (Eq. 1):

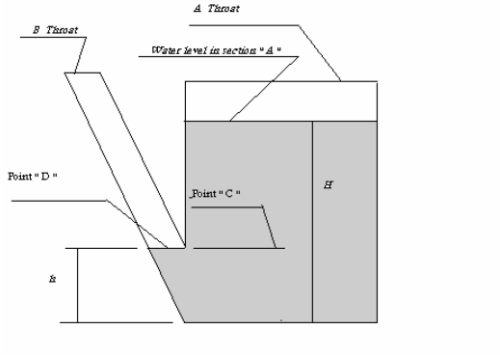

Fig. 6: Equilibrium of pressure in "C" and "D" points

$$P_C = P_D \quad (1)$$

The formula for calculating the hydrostatic pressure of a column of liquid in SI units is (Eq. 2):

$$P_2 = \rho g h + P_{1.} \quad (2)$$

On the other hand the pressure of point "C" can be written as follows (Eq. 3):

$$P_C = (H - h)\rho g + P_{atm.} \quad (3)$$

Then (Eq. 4):

$$P_D = (H - h)\rho g + P_{atm.} \quad (4)$$

According to equation (3), it is obvious that the more the H, the more the P_D (because the height of "h" is constant). Suddenly removing the cork from (B) throat, the pressure due to the difference between "H" and "h" causes the water rises the (B) tube rapidly[1,2].

5 Discussion

Perceiving the above analysis, it can be considered that the recommended hydrostatic system is able to save the potential energy. For increasing the value of this energy, P_D should be increased by adding the value of the difference between "H" and "h". In this way, water can exit out of tube (B) with high speed.

As we know, the potential energy of water in the back of dams is utilized to produce electricity. So, using the above recommended hydrostatic system, we can reuse the water exiting out of turbines in power plants.

It should be noted that we can improve the ability of this recommended hydrostatic system by reducing the diameter of tube (B) for increasing the propulsion of water.

References

[1] Blatt, F. J., (1989). Principles of physics. John Wiley & Sons, Inc., New York, Chapter 11.

[2] Cutnell,J. D. and K. W. Johnson, (1995). Physics (3rdd Edition, John Wiley & Sons, Inc.),314-320

[3] http://www.sensorsone.co.uk/pressure-measurement-glossary/hydrostatic-pressure.html

El Niño and La Niña, Children of the Tropics in Persian Gulf

Maryam Sadat Masoudian, Tehran/ Iran

ARTICLE INFO

Participated and was awarded in First Step to Nobel Prize as high school student (2006-2007)

Accepted in country selection by Ariaian Young Innovative Minds Institute , AYIMI

http://www.ayimi.org ,info@ayimi.org

ABSTRACT

As we know the weather is going to be hot so the worst hurricanes, floods and other bad and new events will happen. In this work, attempt was made to study El Nino and La Nina in Persian Gulf. Iran is a country with normal weather and El Nino and La Nina will happen in areas that have abnormal changeable weather.

Key Words : *El Nino, La Nina, Persian Gulf, hurricanes*

1 Introduction

El Niño is an oscillation of the ocean-atmosphere system in the tropical Pacific having important consequences for weather around the globe. El Nino is a shift in ocean temperatures and atmospheric conditions in the tropical Pacific that disrupts weather around the world (Fig.1). It is a poorly understood recurrent climatic phenomenon that primarily affects the Pacific coast of South America, but has dramatic impacts on weather patterns all over the world.

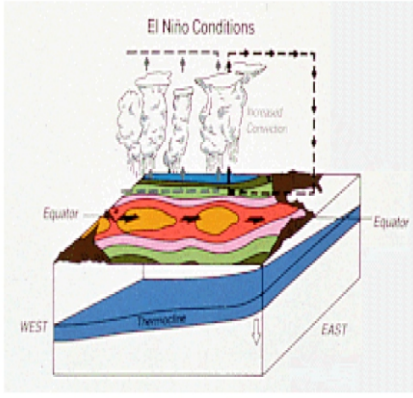

Fig 1: El Nino condition

Pronounced 'El -Nino', it means 'the boy' in Spanish and was named so by Peruvian fishermen after the Christ child since its effects are generally first felt around Christmas. It is a periodic warming of the Pacific Ocean that leads to terrible extremes of weather. The precise causes, intensity, and longevity of El Nino are not very well understood. The warm El Nino phase typically lasts for 8–10 months or so.

Normally, trade winds blow towards the west, across the Pacific, pushing warm surface water away from the South American coast towards Australia and The Philippines. Along the Peruvian coast the water is cold and nutrient-rich, supporting high levels of primary productivity, diverse marine ecosystems, and major fisheries. During El Nino, the trade winds relax in the central and western Pacific. This allows warm water to accumulate in the surface, which causes the nutrients produced by the upwelling of cold water to significantly come down, leading to the killing of plankton and other aquatic life such as fish and the starvation of many sea birds. This is called the El Nino effect, which is also responsible for destructive disruptions of worldwide weather part.

In the 1500s, fishermen who lived in South America began to wonder about a current of unusually warm water that came to their shore every few years near Christmastime. Since the fishermen believed in the birth of the Christ child at Christmas, and since they spoke Spanish, they named the hot water El Nino, which means "the infant" in Spanish.

2 Where Do Scientists Look for El Niño?

The hot water usually comes first to the coasts of Peru and Ecuador in South America. But if we have known about El Niño for four hundred years, why is everyone talking so much about the hot water this year? The 1997-1998 El Niño may or may not be stronger than ever before. Scientists are still deciding. One thing that is definitely different about this El Niño is the technology that scientists are using to study it. Scientists and governments from around the world—United States, France, Japan, Korea and Taiwan are sharing knowledge and funding for The Tropical Atmosphere Ocean (TAO) array. When 1998 began, East Africa should have been at its most beautiful. Normally the short rainy season ends in December, the rivers subside, and the country sparklers; farmers raise crops, animals graze, tourists go on safaris. But this year was different. The rains were heavy and long. The water spread out for miles in places in Kenya and Somalia, cutting off villages and forcing herders to crowd with their livestock onto a few patches of dry land. Things quickly turned ugly. Camels, cows, sheep, and goats all started dying of violent fevers. Soon people, too, began to get sick. Some went temporarily blind; others began bleeding uncontrollably.

The disease was Rift Valley fever, caused by an obscure mosquito-borne virus. It pops up every few years in Africa when standing water encourages mosquito eggs to hatch. This year's huge flood brought a spectacular outbreak: according to official (albeit rough) estimates, at least 89,000 people caught the disease. Two hundred died, but then the disease is not usually fatal to humans. Animal losses, however, were almost certainly vast--owners

probably the worst outbreak of Rift Valley fever in recorded history," says Ali Khan, a medical epidemiologist at the Centers for Disease Control and Prevention in Atlanta. Yet catastrophic as the East African floods were, they had to jostle for the world's attention with other cases of strange weather with unusual occurrences of droughts, fires, rains, cold snaps, and heat waves. Every year brings its own grab bag of such anomalies, but this year many of them could be linked to a phenomenon in the empty expanses of the equatorial Pacific--a change in the ocean currents and winds that began in the early months of 1997 and that altered weather patterns around the world. The change in the weather was, of course, the work of El Nino.

By the end of 1997, El Nino had already become a celebrity of sorts--in storm-battered California, television news programs offered a tabloid flurry of El Nino updates. In 1998, however, El Nino's effects on the world came into full flower. It helped make the year the hottest ever recorded. In addition to Rift Valley fever, El Nino has been linked to an upsurge in diseases ranging from cholera to malaria to dengue fever, in Kenya, Cambodia, Peru, and other countries scattered around the globe. Scientists are now trying to figure out how they can use this year's experiences to predict what the future will bring--both in the next few months and in future decades. The good news is that they can now forecast an El Nino with some precision, and during El Nino years predict its effect on the world's weather months in advance. The bad news is that according to some research this latest El Nino might be a preview of the weather to come in the next century El Nino is caused by an erratically swinging pendulum made of air and water. Under typical conditions a giant pool of warm water sits in the tropical western Pacific.

The heat makes the seawater evaporate and build massive thunderclouds. As rain falls from the clouds, the air both dries out and is pulled upward by the storm's violent updrafts; when the air reaches higher altitudes, it gets blown eastward, until it sinks back down off the coast of South America. This dry air is now blown back west over the Pacific by trade winds, replacing the air carried up and away by the thunderstorms. This cycle is similar to ones found all along the equator, all powered by thunderstorms rising over warm water or on the edges of mountain ranges, and all rotating side by side like a set of interlocking cogs. In the Pacific the atmosphere and the ocean normally reinforce this circulation pattern. As the trade winds travel west, they push the warm surface water of the ocean ahead of them toward the warm pool, making the pool even warmer. As a result of the winds, sea level in the warm pool is actually a few inches higher than in the eastern Pacific. Meanwhile, off the coast of South America, cold water from the deep ocean wells up to replace the surface water pushed west by the trade winds, creating an even bigger temperature difference between the two ends of the ocean. Loaded with nutrients, these upwelling waters support the healthy stocks of fish that Peruvians have depended on for centuries.

3 When Does an El Nino Arrive?

El Nino arrives when the pendulum begins to swing away from this arrangement. Every three to seven years or so, the easterly winds die down. The warm pool is no longer penned in its western Pacific corral and can spread east along the equator. Less cold water rises from the deep along South America; without it, the ocean surface warms even more. With less of a temperature difference between the eastern and western Pacific, the trade winds decrease yet further. That lets the warm pool push farther east. Eventually this collapse of the old arrangement looses a colossal underwater wave of warm water, which races across the ocean until it slams into South America brief.

El Nino is thought to occur due to changes in the normal patterns of trade wind circulation. Normally, these winds move westward, carrying warm surface water to Indonesia and Australia and allowing cooler water to up-well along the South American coast. For reasons not yet fully understood, these trade winds can sometimes be reduced, or even reversed. This moves warmer waters toward the coast of South America and raises water temperatures. Warmer water causes heat and moisture to rise from the ocean off Ecuador and Peru, resulting in more frequent storms and torrential rainfall over these normally arid countries(Figs.2 and 3).

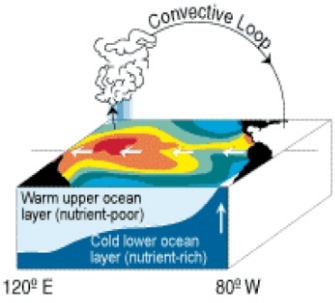

Fig2: Normal condition

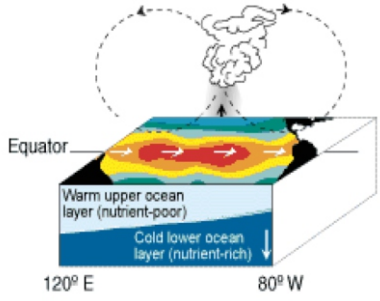

Fig 3: El Niño conditions

4 Why El Niño Occurs and What is La Niña?

La Niña is characterized by unusually cold ocean temperatures in the equatorial Pacific, as compared to El Niño, which is characterized by unusually warm ocean temperatures in the equatorial Pacific.

El Niño and La Niña events vary in strength. For example, the La Niña in 1988 was stronger than the La Niña in 1995, and the 1997-1998 El Niño is unusually strong.

La Niña impact on the global climate: In the U.S., winter temperatures are warmer than normal in the Southeast, and cooler than normal in the Northwest.

Global climate La Niña impacts tend to be opposite those of El Niño impacts. In the tropics, ocean temperature variations in La Niña tend to be opposite those of El Niño.

At higher latitudes, El Niño and La Niña are among a number of factors that influence climate.

However, the impacts of El Niño and La Niña at these latitudes are most clearly seen in wintertime. In the continental US, during El Niño years, temperatures in the winter are warmer than normal in the North Central States, and cooler than normal in the Southeast and the Southwest. During a La Niña year, winter temperatures are warmer than normal

year, winter temperatures are warmer than normal in the

in the Southeast and cooler than normal in the Northwest. An anomaly is the value observed during El Niño or La Niña subtracted from the value in a normal year La Niña means The Little Girl. La Niña is sometimes called El Viejo, anti-El Niño, or simply "a cold event" or "a cold episode".

5 Experiment

Instructions:

Fill one cup with cool water. Fill the other with hot water. (Not boiling, just good and hot.) Place them on a table. Hold each of your hands over one cup and feel the difference in the air above the water.

(Don't actually touch the water. Just feel the air.) The hot water warms the air above it but the cool water doesn't.

Now, fill your bathtub with hot water. Think about how warm and steamy the air in the bathroom gets. Now, imagine millions and millions of bathtubs-full of hot water. All of that moist, hot air has to go somewhere. Scientists know that hot air rises and carries the moisture with it. Once the moisture gets into the air and starts to cool, rain clouds start to form. Then hold a small mirror over the cup of hot water for a few minutes. The moisture in the air should collect on the mirror, and, as it cools, form tiny droplets. Imagine the bathroom mirror after filling the bathtub with hot water. The "water" on the mirror is caused by the water vapor in the air gathering and cooling. Now imagine the air over the hot water of the tropical Pacific Ocean. Huge rain clouds start to form and flooding results in South American countries along the coast.

6 What is the Relationship between Coral Bleaching and El Niño / La Niña?

Coral bleaching results when sea temperature rises above a threshold (about 28C) beyond which corals expel colorful symbiotic algae (hence the bleaching). Deprived of metabolic by-products generated by algae for extended periods, corals die.

Coral bleaching was particularly pronounced during 1997-98 because a very strong El Niño occurred that year and the El Niño related rises in sea temperature were superimposed on a slow upward seatemperature warming trend in some parts of the Pacific and Indian Oceans that may be linked to global warming.

7 What is the Relationship between Greenhouse Warming, El Niño / La Niña and Climate Prediction?

There is a lot of confusion in the public about the interrelations connecting climate phenomena such as El Niño, La Niña and greenhouse effect. Is it true that a warmer atmosphere is likely to produce stronger or more frequent El Niños? It is certainly a plausible hypothesis that global warming may affect El Niño, since both phenomena involve large changes in the earth's heat balance. However, computer climate models, one of the primary research tools for studies of global warming, are hampered by inadequate representation of many key physical processes (such as the effects of clouds on climate and the role of the ocean). Also, no computer model yet can reliably simulate both El Niño and greenhouse gas warming together.

So, depending on which model you choose to believe, you can get different answers. For example, some scientists have speculated that a warmer atmosphere is likely to produce stronger or more frequent El Niños, based on trends observed over the past 25 years. However, some computer models indicate El Niños may actually be weaker in warmer climates.

8 Average El Niño and La Niña

El Niño is characterized by a large scale weakening of the trade winds and warming of the surface layers in the Equatorial eastern and central Pacific Ocean. El Niño events occur irregularly at intervals of 2-7 years, although the average has been, until recently, about once every 3-4 years and lasting 12-18 months. Winters are generally warmer than normal in the northern half of the US. During El Niño years, there are fewer hurricanes in the Atlantic (Figs.4 and 5).

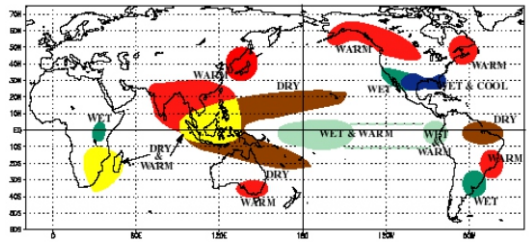

Fig 4: Average El Niño Winters Worldwide

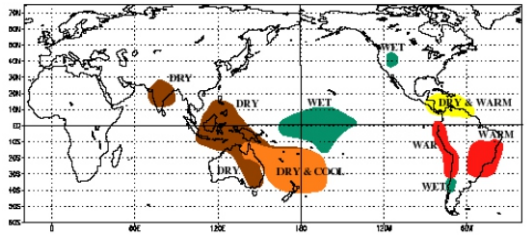

Fig 5: Average El Niño Summers Worldwide

There has been a confusing range of use for the term "El Niño" by both the scientific community and the general public. Originally, the term El Niño denoted a warm southward-flowing ocean current that occurred every year around Christmas off the west coast of Peru and Ecuador. The term was later restricted to an unusually strong warming that disrupted local fish and bird populations every few years. However, as a result of the frequent association of South American coastal temperature anomalies with inter annual basin-scale equatorial warm events. El Niño has also become synonymous with larger scale, climatically-significant, warm events.

9 What is the Relationship between Hurricanes and El Niño?

It is believed that El Niño conditions suppress the development of tropical storms and hurricanes in the Atlantic; and that La Niña (cold conditions in the equatorial Pacific) favor hurricane formation. The world expert in this area of study is Prof. Bill Gray of Colorado State University. Please see their Web pages, including. Conversely, La Niña is the cold counterpart of El Niño where sea surface temperatures in the tropical Pacific fall below normal. This phase is characterized by warm winters in the southeastern United States, colder-than-normal winters from the Pacific Northwest to the Great Lakes, and unsettled winters in the Northeast and Mid-Atlantic states.

Could the problem of disentangling the many factors and dynamics at play in El Niño and global warming can be compared to writing down the scores of many different tunes whilst they are played all at the same time. Might cacophony be a good image to describe circulation patterns?

That's a nice analogy. However, it could be refined in the following way: when the scores are played together, they not only become entangled, but they may actually metamorphose into a slightly different tune, one for which no score existed at the start of the piece. That is to say, that El Nino, global warming, and other climate signals are actually physically altered by their interaction in ways you would not expect by considering them in isolation. Sorting out these complex interactions is in fact one of the major challenges of climate research today.

At higher latitudes, El Niño is only one of a number of factors that influence climate. However, the impacts of El Niño and La Niña at these latitudes are most clearly seen in wintertime. In the continental US, during El Niño years, temperatures in the winter are warmer than normal in the North Central States, and cooler than normal in the Southeast and the Southwest. During a La Niña or El Viejo year, winter temperatures are warmer than normal in the Southeast and cooler than normal in the Northwest El Niño and La Niña are opposite phases of the El Niño-Southern Oscillation (ENSO) cycle, with La Niña sometimes referred to as the cold phase of ENSO and El Niño as the warm phase of ENSO (Figs. 6 and 7).

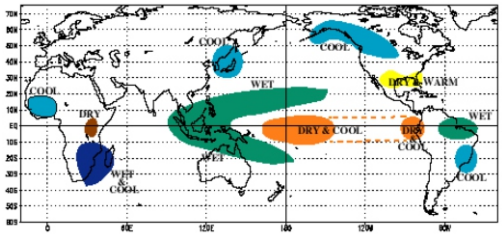

Fig 6 : Average La Niña Winters Worldwide

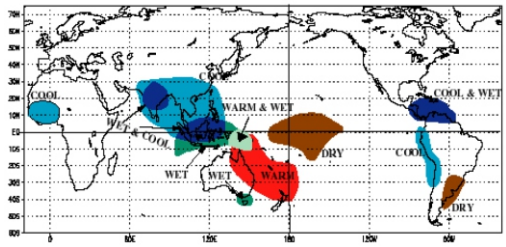

Fig 7: Average La Niña Summers Worldwide

9 Persian Gulf

In this work, attempt was made to study El Nino and La Nina in Persian Gulf. As it shown, you can understand that Iran has normal weather and El Nino and La Nina occur in hot or cold lands. As a result you can recognize that El Nino will happen when the temperature increased from its normal in a distinguished season .It is obvious about La Nina. The maximum and minimum temperature of Persian Gulf are shown in Table (1).

Table 1: Temperature in Persian Gulf

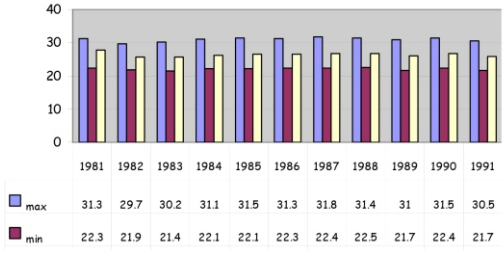

The maximum temperature was in 1987 (31.5) and the minimum was in 1983(21.3).As you can see there was a little change between the temperature from the year 1981 until 1991 and hurricanes happen when the temperature increases or decreases a lot. SO it hasn't happen yet but will occur later because of increasing temperature of the world.

We invite all who are interested to send their research to Young Scientist Research Journal according to the template .
All related author's guidelines are in http://journal.ayimi.org.

Ariaian Young Innovative Minds Institute, AYIMI
Unit 14, No. 32, Malek Ave., Shariati St.
Post Code: 1565843537
Tel - Fax: +9821-77522395, 77507013
Tehran/ Iran
URL: http://www.ayimi.org
http://journal.ayimi.org
Email: info@ayimi.org